

1 Geoderma

2

3 Title: Integration of mid-infrared spectroscopy and geostatistics in the assessment of soil  
4 spatial variability at landscape level

5

6 Article Type: Research Paper

7

8 Section/Category: Soil Fertility, Soil Quality and Tropical Soils

9

10 Keywords: Autocorrelation; chemometrics; DRIFT; sampling designs; soil fertility; spatial  
11 patterns; variography; Zimbabwe.

12

13 Corresponding Author: Dr. G. Cadisch,

14

15 Corresponding Author's Institution: Uni Hohenheim

16

17 First Author: Juan Guillermo Cobo

18

19 Order of Authors: Juan Guillermo Cobo; Gerd Dercon; Tsitsi Yekeye; Lazarus Chapungu;  
20 Chengetai Kadzere; Amon Murwira; Robert Delve; G. Cadisch

21

22 Abstract: Knowledge of soil spatial variability is important in natural resource management,  
23 interpolation and soil sampling design, but requires a considerable amount of geo-referenced  
24 data. In this study, mid-infrared spectroscopy in combination with spatial analyses tools is  
25 being proposed to facilitate landscape evaluation and monitoring. Mid-infrared spectroscopy

26 (MIRS) and geostatistics were integrated for evaluating soil spatial structures of three land  
27 settlement schemes in Zimbabwe (i.e. communal area, old resettlement and new resettlement;  
28 on loamy-sand, sandy-loam and clay soils, respectively). A nested non-aligned design with  
29 hierarchical grids of 750, 150 and 30 m resulted in 432 sampling points across all three  
30 villages (730-1360 ha). At each point, a composite topsoil sample was taken and analyzed by  
31 MIRS. Conventional laboratory analyses on 25-38% of the samples were used for the  
32 prediction of concentration values on the remaining samples through the application of MIRS  
33 - partial least squares regression models. These models were successful ( $R^2 > 0.89$ ) for sand,  
34 clay, pH, total C and N, exchangeable Ca, Mg and effective CEC; but not for silt, available P  
35 and exchangeable K and Al ( $R^2 < 0.82$ ). Minimum sample sizes required to accurately estimate  
36 the mean of each soil property in each village were calculated. With regard to locations,  
37 fewer samples were needed in the new resettlement area than in the other two areas (e.g. 66  
38 versus 133-473 samples for estimating soil C at 10% error, respectively); regarding  
39 parameters, less samples were needed for estimating pH and sand (i.e. 3-52 versus 27-504  
40 samples for the remaining properties, at same error margin). Spatial analyses of soil  
41 properties in each village were assessed by constructing standardized isotropic  
42 semivariograms, which were usually well described by spherical models. Spatial  
43 autocorrelation of most variables was displayed over ranges of 250-695 m. Nugget-to-sill  
44 ratios showed that, in general, spatial dependence of soil properties was: new resettlement >  
45 old resettlement > communal area; which was potentially attributed to both intrinsic (e.g.  
46 texture) and extrinsic (e.g. management) factors. As a new approach, geostatistical analysis  
47 was performed using MIRS data directly, after principal component analyses, where the first  
48 three components explained 70% of the overall variability. Semivariograms based on these  
49 components showed that spatial dependence per village was similar to overall dependence  
50 identified from individual soil properties in each area. In fact, the first component (explaining

51 49% of variation) related well with all soil properties of reference samples (absolute  
52 correlation values of 0.55-0.96). This suggested that MIRS data could be directly linked to  
53 geostatistics for a broad and quick evaluation of soil spatial variability. It is concluded that  
54 integrating MIRS with geostatistical analyses is a cost-effective promising approach, i.e. for  
55 soil fertility and carbon sequestration assessments, mapping and monitoring at landscape  
56 level.

57 **Integration of mid-infrared spectroscopy and geostatistics in the assessment of soil**  
58 **spatial variability at landscape level**

59

60 **Juan Guillermo Cobo<sup>1,2</sup>, Gerd Dercon<sup>1,3</sup>, Tsitsi Yekeye<sup>4</sup>, Lazarus Chapungu<sup>4</sup>, Chengetai**  
61 **Kadzere<sup>2</sup>, Amon Murwira<sup>4</sup>, Robert Delve<sup>2,5</sup>, Georg Cadisch<sup>1,\*</sup>**

62 *<sup>1</sup> University of Hohenheim, Institute of Plant Production and Agroecology in the Tropics and*  
63 *Subtropics, 70593 Stuttgart, Germany*

64 *<sup>2</sup> Tropical Soil Biology and Fertility Institute of the International Center for Tropical*  
65 *Agriculture (TSBF-CIAT), MP 228, Harare, Zimbabwe*

66 *<sup>3</sup> Present address: Soil and Water Management and Crop Nutrition Subprogramme, Joint*  
67 *FAO/IAEA Division of Nuclear Techniques in Food and Agriculture, Department of Nuclear*  
68 *Sciences and Applications, International Atomic Energy Agency – IAEA, Wagramerstrasse 5*  
69 *A-1400, Vienna, Austria*

70 *<sup>4</sup> University of Zimbabwe, Dept. of Geography and Environmental Science, MP 167*  
71 *Harare, Zimbabwe*

72 *<sup>5</sup> Present address: Catholic Relief Services, P.O. Box 49675-00100, Nairobi, Kenya*

73

74

75 Pages: 27

76 Figures: 10

77 Tables: 4

78

79

80 \* Corresponding author: E-mail address: [georg.cadisch@uni-hohenheim.de](mailto:georg.cadisch@uni-hohenheim.de); Tel.: +49 711

81 459 22438; Fax: +49 711 459 22304.

82 **Abstract**

83 Knowledge of soil spatial variability is important in natural resource management,  
84 interpolation and soil sampling design, but requires a considerable amount of geo-referenced  
85 data. In this study, mid-infrared spectroscopy in combination with spatial analyses tools is  
86 being proposed to facilitate landscape evaluation and monitoring. Mid-infrared spectroscopy  
87 (MIRS) and geostatistics were integrated for evaluating soil spatial structures of three land  
88 settlement schemes in Zimbabwe (i.e. communal area, old resettlement and new resettlement;  
89 on loamy-sand, sandy-loam and clay soils, respectively). A nested non-aligned design with  
90 hierarchical grids of 750, 150 and 30 m resulted in 432 sampling points across all three  
91 villages (730-1360 ha). At each point, a composite topsoil sample was taken and analyzed by  
92 MIRS. Conventional laboratory analyses on 25-38% of the samples were used for the  
93 prediction of concentration values on the remaining samples through the application of MIRS  
94 - partial least squares regression models. These models were successful ( $R^2 > 0.89$ ) for sand,  
95 clay, pH, total C and N, exchangeable Ca, Mg and effective CEC; but not for silt, available P  
96 and exchangeable K and Al ( $R^2 < 0.82$ ). Minimum sample sizes required to accurately estimate  
97 the mean of each soil property in each village were calculated. With regard to locations,  
98 fewer samples were needed in the new resettlement area than in the other two areas (e.g. 66  
99 versus 133-473 samples for estimating soil C at 10% error, respectively); regarding  
100 parameters, less samples were needed for estimating pH and sand (i.e. 3-52 versus 27-504  
101 samples for the remaining properties, at same error margin). Spatial analyses of soil  
102 properties in each village were assessed by constructing standardized isotropic  
103 semivariograms, which were usually well described by spherical models. Spatial  
104 autocorrelation of most variables was displayed over ranges of 250-695 m. Nugget-to-sill  
105 ratios showed that, in general, spatial dependence of soil properties was: new resettlement >  
106 old resettlement > communal area; which was potentially attributed to both intrinsic (e.g.

107 texture) and extrinsic (e.g. management) factors. As a new approach, geostatistical analysis  
108 was performed using MIRS data directly, after principal component analyses, where the first  
109 three components explained 70% of the overall variability. Semivariograms based on these  
110 components showed that spatial dependence per village was similar to overall dependence  
111 identified from individual soil properties in each area. In fact, the first component (explaining  
112 49% of variation) related well with all soil properties of reference samples (absolute  
113 correlation values of 0.55-0.96). This showed that MIRS data could be directly linked to  
114 geostatistics for a broad and quick evaluation of soil spatial variability. It is concluded that  
115 integrating MIRS with geostatistical analyses is a cost-effective promising approach, i.e. for  
116 soil fertility and carbon sequestration assessments, mapping and monitoring at landscape  
117 level.

118

#### 119 **Key words**

120 Autocorrelation; chemometrics; DRIFT; sampling designs; soil fertility; spatial patterns;  
121 variography; Zimbabwe.

122

#### 123 **1. Introduction**

124 Soil properties are inherently variable in nature mainly due to pedogenetical factors (e.g.  
125 parental material, vegetation, climate), but heterogeneity can be also induced by farmers'  
126 management (Dercon et al., 2003; Giller et al., 2006; Samake et al., 2005; Wei et al., 2008;  
127 Yemefack et al., 2005). Soil spatial variability can occur over multiple spatial scales, ranging  
128 from micro-level (millimeters), to plot level (meters), up to the landscape (kilometers)  
129 (Garten Jr. et al., 2007). Thus, soil spatial variability is a function of the different driving  
130 factors and spatial scale (in terms of size and resolution), but also of the specific soil property  
131 (or process) under evaluation and the spatial domain (location), among others factors (Lin et

132 al., 2005). Recognizing spatial patterns in soils is important as this knowledge can be used for  
133 enhancing natural resource management (e.g. Borůvka et al., 2007; Liu et al., 2004; Wang et  
134 al., 2009), predicting soil properties at unsampled locations (e.g. Liu et al., 2009; Wei et al.,  
135 2008) and improving sampling designs in future agro-ecological studies (e.g. Rossi et al.,  
136 2009; Yan and Cai, 2008). In fact, the identification of spatial patterns is the first step to  
137 understanding processes in natural and/or managed systems, which are usually characterized  
138 by spatial structures due to spatial autocorrelation: i.e. where closer observations are more  
139 likely to be similar than by random chance (Fortin et al., 2002). Conventional statistical  
140 analyses are not appropriate to identify spatial patterns, as these analyses require the  
141 assumption of independence among samples, which is violated when auto-correlated  
142 (spatially dependent) data are present (Fortin et al., 2002; Liebhold and Gurevitch, 2002).  
143 Thus, since 1950s, alternative methods, so-called spatial statistics, have been developed for  
144 dealing with spatial autocorrelation (Fortin et al., 2002). Today several methods for spatial  
145 analyses exist (e.g. Geostatistics, Mantel tests, Moran's I, Fractal analyses), while the reasons  
146 for the different studies carried out to date on spatial assessments are also diverse (e.g.  
147 hypotheses testing, spatial estimation, uncertainty assessment, stochastic simulation,  
148 modeling) (Goovaerts, 1999; Liebhold and Gurevitch, 2002). However, a common  
149 characteristic is that all methods intent to capture and quantify in one way or another  
150 underlying spatial patterns of a specific spatial domain (Liebhold and Gurevitch, 2002; Olea,  
151 2006).

152

153 Geostatistics is one of the most used and powerful approaches for evaluating spatial  
154 variability of natural resources such as soils (Sauer et al., 2006). However, construction of  
155 stable semivariograms (the main tool on which geostatistics is based) requires considerable  
156 amount of geo-referenced data (Davidson and Csillag, 2003). Infrared spectroscopy (IRS) has

157 been suggested as a viable option to facilitate access to the extensive soil data required  
158 (Cécillon et al., 2009; Shepherd and Walsh, 2007). IRS is able to detect the different  
159 molecular vibrations due to the stretching and binding of the different compounds of a sample  
160 when illuminated by an infrared beam in the near, NIRS (0.7-2.5  $\mu\text{m}$ ), or mid, MIRS (2.5-25  
161  $\mu\text{m}$ ) ranges. The result of the measurements is summarized in one spectrum (e.g. wavelength  
162 versus absorbance), which is later related by multivariate calibration to known concentration  
163 values of the properties of interest (e.g. carbon content, texture) from reference samples.  
164 Thus, a mathematical model is created and used later for the prediction of concentration  
165 values of these properties in other samples from which IRS data is also available (Conzen,  
166 2003). IRS measurements are therefore not destructive, take few minutes, and one spectra can  
167 be related to multiple physical, chemical and biological soil properties (Janik et al., 1998;  
168 McBratney et al., 2006). Hence the technique is more rapid and cheaper than conventional  
169 laboratory analysis, especially when a large number of samples must be analyzed (Viscarra-  
170 Rossel et al., 2006). IRS has the additional advantage that spectral information can be used as  
171 an integrative measure of soil quality, and therefore employed as a screening tool of soil  
172 conditions (Shepherd and Walsh, 2007). The few existing initiatives in this regard are,  
173 however, limited to NIRS. For example, a visible-NIRS (VNIRS) soil fertility index based on  
174 ten common soil properties has been developed and applied in Madagascar (Vågen et al.,  
175 2006); ordinal logistic regression and classification trees were used to discriminate soil  
176 ecological conditions by using biogeochemical data and VNIRS in the USA (Cohen et al.,  
177 2006); and in Kenya, Awiti et al. (2008) developed an odds logistic model based on principal  
178 components from NIRS for soil fertility classification. Nevertheless, despite its multiple  
179 applications, to date IRS has not been widely used, especially for wide-scale purposes and in  
180 developing countries (Shepherd and Walsh, 2007).

181



182 African regions are usually characterized by food insecurity and poverty, which have been  
183 extensively attributed to low soil fertility and soil mining (Sanchez and Leakey, 1997;  
184 Vitousek et al., 2009). Therefore, to boost land productivity in the continent, there is an  
185 increasing need to develop and apply reliable indicators of land quality at different spatial  
186 scales (Cobo et al., 2010). In fact, Shepherd and Walsh (2007) proposed that the successful  
187 “combination of infrared spectroscopy and geographic positioning systems will provide one  
188 of the most powerful modern tools for agricultural and environmental monitoring and  
189 analysis” in the next decade. The present study aims to contribute to this goal, and follows up  
190 a study from Cobo et al. (2009), in which three villages as typical cases of three settlement  
191 schemes in north-east Zimbabwe (communal area, old resettlement and new resettlement)  
192 were evaluated to determine specific cropping strategies, soil fertility investments and land  
193 management practices at each site. The assessment, however, was done at plot and farm level,  
194 and did not take into account spatial structures of soil properties. Hence, the same three  
195 villages of Cobo et al. (2009) were systematically sampled, soils characterized by MIRS, and  
196 data subsequently analyzed using conventional statistics and geostatistics tools. The main  
197 objectives of this study were: i) to evaluate advantages and disadvantages of using MIRS and  
198 geostatistics in the assessment of spatial variability of soils, ii) to test if MIRS can be directly  
199 integrated with geostatistics for landscape analyses, and iii) to present recommendations for  
200 guiding future sampling designs.

201

## 202 **2. Materials and methods**

### 203 *2.1 Description of study sites*

204 The study sites consisted of three villages, selected as typical cases of three small-holder  
205 settlement schemes, in the districts of Bindura and Shamva, north-east Zimbabwe (Table 1).

206 The first village, Kanyera, is located in a communal area, covers 730 ha, and is mainly

207 characterized with loamy sand soils of low fertility. The second village, Chomutomora, is  
208 located in an old resettlement area (from 1987), covers 780 ha and mostly presents sandy  
209 loam soils of low quality. The third village, Hereford farm, is located in a new resettlement  
210 area (from 2002), covers 1360 ha and is predominantly characterized by clay soils of  
211 relatively higher fertility. All villages are located in natural region II, which covers a region  
212 with altitudes of 1000 to 1800 m a.s.l. and unimodal rainfall (April to October) with 750–  
213 1000 mm per annum (FAO, 2006). Maize (*Zea maiz* L.) is the main crop planted in the three  
214 areas, and farmers have free access to communal grazing areas and woodlands. A full  
215 description of the sites' selection and characteristics is provided in Cobo et al. (2009).

216

## 217 2.2. Soil sampling design

218 A non-aligned block sampling design was used in the three villages to capture both small and  
219 large variation over large areas (Urban, 2002). It started with the delineation of the villages'  
220 boundaries by using a hand-held GPS. Coordinates were later overlaid in ArcView  
221 ([www.esri.com](http://www.esri.com)) to a Landsat TM image of the zone acquired on 12 June 2006. A buffer of 30  
222 m inside each village boundary was created and later a grid of 750 x 750 m was drawn for  
223 each village in ILWIS ([www.ilwis.org](http://www.ilwis.org)) (Figure 1a). Next, each main cell of 750 x 750 m was  
224 divided in 25 sub-cells of 150 x 150 m, which were subsequently divided once again in 25  
225 micro-cells of 30 x 30 m. All grids were later transferred to ArcView, where 3 sub-cells from  
226 each main cell and 3 micro-cells from each sub-cell were randomly selected. This yielded a  
227 cluster of 9 micro-cells per main cell (Figure 1b). Finally, the centroids of each selected  
228 micro-cells were estimated and included into the GPS to locate these points in the field  
229 (Figure 1c). However, as some points were found in unsuitable places for sampling (e.g. road,  
230 water way, household) they were re-located (if possible) to alternate locations within  
231 cropping fields, grasslands or woodlands, mostly inside a radius of 30 m. In the same way, in

232 cropping fields maize was preferentially chosen for future comparison purposes. At Hereford  
233 farm, a part of the woodlands in the southern border was considered to be sacred by the  
234 villagers, hence this sector was excluded. 432 points were successfully sampled in the three  
235 villages: 159 points in cropping fields (105 in maize, 32 in fallow and 22 in other crops), 163  
236 in woodlands and 110 in grasslands. Maximum sampling distance between points was 5.2  
237 (communal area), 3.8 (old resettlement) and 4.6 km (new resettlement); while minimum  
238 sampling distance was 30 m (for all three villages). Sample collection was carried out at the  
239 end of the 2006-7 cropping season.

240

241 Each sampling point consisted of a radial-arm containing four sampling plots: one central and  
242 other three located at 12.2 m in directions north, south-west and south-east (Figure 1d), which  
243 were designed to represent the internal characteristics and variations in each 30 x 30 m  
244 micro-cell (K. Shepherd & T. Vågen, personal communication, 2006). Once plots were  
245 established, they were fully characterized by using the FAO land cover classification system  
246 (FAO, 2005). Soils were sampled (0-20 cm depth) in each plot and all soil samples per point  
247 (4 plots) were thoroughly mixed to account for short-range (<30 m) spatial variability, and a  
248 composite sub-sample (~250 g) was taken from the field. Composite soil sub-samples were  
249 air-dried, sieved (<2 mm) and a sub-sub-sample sent to Germany for laboratory analyses.

250

### 251 *2.3. Conventional and MIRS analyses of soil samples*

252 Soil texture, pH, total carbon (C) and nitrogen (N), available phosphorus ( $P_{av}$ ), exchangeable  
253 potassium (K), calcium (Ca), magnesium (Mg) and aluminum (Al), and effective cation  
254 exchange capacity (CEC) were analyzed on 25% (texture) to 38% (other soil properties) of all  
255 collected samples (referred in this study as “reference samples”) for the calibration and  
256 validation of the MIRS models. Soil texture was determined by Bouyucos (Anderson and

257 Ingram, 1993), pH by  $\text{CaCl}_2$  (Anderson and Ingram, 1993), total C and N by combustion  
258 using an auto-analyzer (EL, Elementar Analysensysteme, Germany),  $P_{\text{av}}$  by the molybdenum  
259 blue complex reaction method of Bray and Kurtz (1945) and exchangeable cations and  
260 effective CEC by extraction with ammonium chloride (Schöning and Brümmer, 2008).  
261  
262 All 432 soil samples were analyzed by Diffuse Reflectance Infrared Fourier Transform  
263 (DRIFT) -MIRS. Five grams of ball-milled soil samples were scanned in a TENSOR-27 FT-  
264 IR spectrometer (Bruker Optik GmbH, Germany) coupled to a DRIFT-Praying Mantis  
265 chamber (Harrick Scientific Products Inc., New York, US). Spectra were obtained at least in  
266 triplicate, from 600 to 4,000 wavenumber  $\text{cm}^{-1}$ , with a resolution of 4  $\text{cm}^{-1}$  and 16  
267 scans/sample, and expressed in absorbance units [ $\log(1/\text{Reflectance})$ ]. Potassium bromide  
268 (KBr) for IR spectroscopy (assay  $\geq 99.5\%$ ), kept always dry in a desiccator, was used as a  
269 background. All spectral replicates per sample were averaged and later subjected to  
270 multivariate calibration by using partial least square (PLS) regression, which relates the  
271 processed spectra (e.g. Figure 2) to the related concentration values from the reference  
272 samples. Through a random split selection of the reference samples, half of the samples were  
273 used for calibration, while the other half left for validation. Chemometric models were  
274 constructed with the “Optimization” function of the OPUS-QUANT2 package (Bruker Optik  
275 GmbH, Germany). Calibration regions were set to exclude the background  $\text{CO}_2$  region (2300-  
276 2400  $\text{cm}^{-1}$ ) and the edge of the detection limits of the spectrometer ( $<700$  and  $>3900$   $\text{cm}^{-1}$ ) to  
277 reduce noise. Prediction accuracy of selected MIRS models was evaluated by the residual  
278 prediction deviation (RPD) value, the coefficient of determination ( $R^2$ ) and the root mean  
279 square error of the prediction (RMSEP). Once suitable chemometric models were selected,  
280 models were applied to every spectrum replicate of non reference samples for the prediction  
281 of unknown concentration values for each possible soil property; and results of all replicates

282 per sample were finally averaged. All spectral manipulation and development of chemometric  
283 models were carried out in OPUS, version 6.5 (Bruker Optik GmbH, Germany).

284

#### 285 *2.4. Conventional statistical analyses*

286 Descriptive statistics were calculated to explore the distribution of each soil property under  
287 evaluation and as a critical step before geostatistical analyses (Olea, 2006). This comprised  
288 the calculation of univariate statistical moments (e.g. mean, median, range), construction of  
289 scatter plots, box plots, frequency tables and normality tests, as well as the identification of  
290 true outliers and their exclusion if necessary, as even a few outliers can produce very unstable  
291 results (Makkawi, 2004). We usually considered as outliers those points with values higher or  
292 lower than three standard deviations from the mean (Liu et al., 2009). The coefficient of  
293 variation (CV) was calculated as an index for assessing overall variability (Gallardo and  
294 Paramá, 2007). The non-parametric tests of Kruskal-Wallis and Mann-Whitney (a Kruskal-  
295 Wallis version for only two levels) were chosen for testing the equality of medians among  
296 villages following the method of Bekele and Hudnall (2006). All classical statistical analyses  
297 were performed in SAS version 9.2 (SAS Institute Inc).

298

#### 299 *2.5. Minimum sample size estimations*

300 The minimum number of samples required for estimating the mean of the different evaluated  
301 soil properties in each village, at different probabilities of its true value (error), with a 95% of  
302 confidence, was estimated by using equation 1:

303

$$304 \quad n = [(t_{\alpha} * s)/d]^2 \quad \text{(equation 1)}$$

305

306 where  $n$  is the sample size,  $t$  is the value of t Student (at  $\alpha=0.05$  and  $n-1$  degrees of freedom,  
307 i.e. 1.96),  $s$  is the standard deviation, and  $d$  is the margin of error (Garten Jr. et al., 2007;  
308 Rossi et al., 2009; Yan and Cai, 2008).

309

## 310 *2.6. Geo-statistical analyses of estimated soil properties*

311 The spatial dependence of soil properties, as determined by the combination of conventional  
312 laboratory analyses and MIRS, was assessed in each area by using geostatistical analyses, via  
313 the semivariogram, which measures the average dissimilarity of data as a function of distance  
314 (Goovaerts, 1999) as illustrated in equation 2:

315

$$316 \quad \gamma(h) = 1/2N(h) \sum_i \sum_{i+h} [z(i)-z(i+h)]^2 \quad (\text{equation 2})$$

317

318 where  $\gamma$  is the semivariance for  $N$  data pairs separated by a distance lag  $h$ ; and  $z$  the variable  
319 under consideration at positions  $i$  and  $i+h$ . As construction of semivariograms assumes a  
320 Gaussian distribution (Olea, 2006; Reimann and Filzmoser, 2000), variables were  
321 transformed if necessary to approximate normality and to stabilize variance (Goovaerts,  
322 1999). Data were also detrended by fitting low-order polynomials according to the exhibited  
323 trend (if existent) to accounting for any systematic variation (i.e. global trend) and hence  
324 fulfilling the assumption of stationarity (Bekele and Hudnall, 2006; Sauer et al., 2006). Thus,  
325 after detrending, respective residuals were used to construct standardized isotropic  
326 semivariograms for each soil property in each village. Hence, anisotropy (effect of direction  
327 in the intensity of spatial dependence) was not taken into account, as this analysis required a  
328 higher number of samples for the construction of stable semivariograms in each direction.  
329 When number of samples is limited an omnidirectional (isotropic) characterization of  
330 spatial dependence is more recommendable (Davidson and Csillag, 2003). The

331 standardization was achieved by dividing the semivariance data by the sample variance, and  
332 this allowed a fair comparison among variables and sites (Pozdnyakova et al., 2005). The half  
333 of the maximum sampling distance in each village was chosen as the active lag distance for  
334 the construction of all semivariograms, and more than 100 pairs per each lag distance class  
335 interval were included in the calculations.

336

337 Once semivariograms were constructed, theoretical semivariogram models were fitted to the  
338 data. This was done by selecting the model with the lowest residual sum of squares and  
339 highest  $R^2$  (e.g. Liu et al., 2009; Wang et al., 2009; Wei et al., 2008). As the spherical model  
340 characterized well most of the cases, this model was selected to fit all data (with the  
341 exception when a linear trend was found). Having the same model further facilitates  
342 comparisons among variables and villages (Cambardella et al., 1994; Davidson and Csillag,  
343 2003; Gallardo and Paramá, 2007). The spherical model is defined in equation 3 (Liu et al.,  
344 2004; Pozdnyakova et al., 2005) as:

345

$$\begin{aligned} 346 \quad \gamma(h) &= \{ Co + C [ 1.5 (h/a) - 0.5(h/a)^3 ] \} & 0 < h \leq a & \quad \text{(equation 3)} \\ 347 \quad &= \{ Co + C & h > a & \end{aligned}$$

348

349 where  $\gamma$  is the semivariance,  $h$  the distance,  $Co$  is the nugget,  $Co+C$  is the sill, and  $a$  is the  
350 range. These parameters were used to describe and compare spatial structures of soil  
351 properties in each village. ArcGIS version 9 (ESRI) and procedures Univariate, Means and  
352 Variogram of SAS version 9.2 were used for exploratory data and trend analyses; while Proc  
353 GLM of SAS was used for data detrending. Construction of semivariograms and model  
354 fitting were performed in GS<sup>+</sup> version 9 (Gamma Design Software, USA).

355

## 356 2.7. Geo-statistical analyses of MIRS data

357 To determine the feasibility of using MIRS data as direct input for the determination of  
358 spatial variation of soils, all spectra were baseline corrected (Rubberband correction method,  
359 64 baseline points) and derived (1<sup>st</sup> order derivative, Savitzky-Golay algorithm, 9 smoothing  
360 points) in OPUS. Data were later exported to SAS, where the CO<sub>2</sub> regions and the edges of  
361 the spectra were excluded, as explained for the multivariate calibration. Next, spectral data  
362 were reduced by re-sampling at 12 cm<sup>-1</sup> and selected wavenumbers (i.e. variables) subjected  
363 to Spearman correlation analyses among each other, where highly autocorrelated variables  
364 (i.e.  $r > 0.99$ ) were manually excluded, to reduce computational demands. Data were later  
365 standardized to zero mean and unit variance, and analyzed by principal component analyses  
366 (Borůvka et al., 2007; Yemefack et al., 2005). The three first components were retained,  
367 rotated (varimax option) and respective scores assigned to each soil sample. Score  
368 components were thus used as input variables for the constructions of semivariograms per  
369 each village, by following the same methodology previously explained for the conventional  
370 soil parameters. Spearman correlation analyses were finally performed between the principal  
371 components and chemical data from reference samples.

372

## 373 3. Results

### 374 3.1. MIRS models and prediction

375 A good representation across the different concentration ranges for most of the soil properties  
376 was obtained by the selection of the samples, as shown in Figure 3. Calibration and validation  
377 models also showed that predictability potential of MIRS varied with the specific soil  
378 property under evaluation and location, as indicated by the different model fit and  
379 performance indicators (Figure 3, Table 2). For example, in agricultural applications RPD  
380 values higher than 5 indicate that predictions models are excellent; RPD values greater than 3



381 are considered acceptable; while values less than 3 indicate poor prediction power (Pirie et  
382 al., 2005). Besides,  $R^2$  values near 1 typically indicate good models (Conzen, 2003), in  
383 particular when bias is minimal and regression line follows the 1:1 line. Hence, excellent  
384 models ( $5 < \text{RPD} \leq 6.8$ ,  $0.96 \leq R^2 \leq 0.98$ ) were obtained for sand, clay, C, N, Ca and CEC;  
385 acceptable models ( $3 < \text{RPD} < 5$ ,  $0.89 < R^2 < 0.92$ ) were obtained for pH and Mg; while  
386 unsuitable models ( $\text{RPD} < 3$ ,  $R^2 \leq 0.82$ ) were obtained for silt,  $P_{\text{av}}$ , K and Al. Poor validation for  
387 these last variables (especially  $P_{\text{av}}$ , K and Al) was the result of a deficient calibration, as  
388 indicated by their model fit (Figure 3) and parameters (Table 2). Mid-infrared spectroscopy  
389 models for these variables were thus not used for prediction, and hence these data were  
390 dropped from any further analyses. Silt fraction, however, could be calculated from the other  
391 two fractions (silt = 100 – sand - clay). Therefore, by using the selected MIRS models shown  
392 in Table 2 for the prediction of soil parameters in non-reference samples, the entire dataset of  
393 sand, silt, clay, pH, C, N, Ca, Mg and CEC could be completed.

394

### 395 *3.2. Exploratory data analysis and differences among villages*

396 Exploratory data analyses in the entire dataset indicated that most soil properties presented  
397 skewed and kurtic distributions (data not shown). For example, texture fractions showed  
398 clearly a bimodal distribution, which suggested the presence of different populations, as it  
399 was in fact the case (i.e. different villages presenting different textural classes). Descriptive  
400 statistics and histograms were therefore also obtained by village. In this case, although  
401 texture fractions often approximated normality, the other soil properties still exhibited non-  
402 normal distributions (data not shown). Non-normality is usually the rule and not the  
403 exception when dealing with geostatistical and environmental data (Reimann and Filzmoser,  
404 2000). This is why the median (instead of the mean) and non-parametric approaches were

405 preferably used for classical statistical analyses, in spite of data transformation of skewed  
406 variables usually helped to approximate normality.

407

408 Overall variability of soil properties in each area was evaluated by its coefficient of variation.  
409 According to Wei et al. (2008), a CV less than 10% indicates that variability of a considered  
410 property is low; while a CV higher than 90% indicates high variation. Thus, calculated CVs  
411 in the entire dataset (Figure 4A) showed that Ca, Mg and CEC were the properties with the  
412 highest overall variability (>90%); while only pH presented a relative low variation (~10%).  
413 Other evaluated soil properties showed intermediate variability (CV=10-90%). When  
414 calculations were performed by village (Figure 4B-D), CVs of all soil properties reduced  
415 considerably, as expected. Data showed that Mg varied the most in the three villages, while  
416 pH (in all villages) and sand (in the communal and old resettlement area) presented the  
417 lowest variation. With the particular exception of sand and pH, variability of all soil  
418 properties in the new resettlement was lower than in the other two areas.

419

420 Differences in medians among villages for all soil properties were significant at  $p < 0.001$   
421 (Figure 5). Differences were especially evident when the communal and old resettlement  
422 areas were compared to the new resettlement area, mainly due to divergent soil textural types  
423 (Table 1). In fact, the new resettlement area presented the lowest values for sand and the  
424 highest for the remaining properties. This is why a Mann-Whitney test was also performed to  
425 compare only between the communal and old resettlement area. This analysis showed highly  
426 significant differences ( $p < 0.001$ ) in medians between these two villages for all evaluated soil  
427 properties (Figure 5).

428

429 *3.3. Minimum sample size requirements*

430 Estimated minimum sample sizes, for all evaluated parameters, exhibited a negative  
431 exponential trend by increasing the margin of error (Figure 6). Taking soil C as an example, a  
432 minimum of 473 samples would be required in the communal area to estimate the mean at  
433 5% of its true value; while a minimum of 118, 53, 30 and 19 samples would be necessary at  
434 margins errors of 10, 15, 20 and 25%, respectively. With the exception of sand and pH, the  
435 required number of samples was found to be lower in the new resettlement area than in the  
436 other villages. In general, a higher number of samples would be required for Mg, CEC and  
437 Ca, while relatively fewer samples would be necessary for pH, silt and sand.

438

#### 439 *3.4. Geostatistical analyses of generated soil data*

440 Geostatistical analyses require data following Gaussian distribution. Thus, transformation of  
441 variables was necessary in most of the cases (see Table 3) and this generally allowed to  
442 approximate normality. However, for Mg in the communal and old resettlement areas any  
443 transformations used could shift the highly skewed distribution of this variable. This was  
444 attributed to the low concentrations measured (Figure 5), where a high proportion of samples  
445 had null values as they were below analytical detection limits. Approximations to normality  
446 in a situation like this is simply not possible by any mean (Reimann and Filzmoser, 2000);  
447 therefore data for Mg must be interpreted with caution for these two areas.

448

449 To determine the grade of spatial dependence of each soil property, the nugget-to-sill ratio  
450 from all semivariograms was calculated. According to Cambardella et al. (1994), and since  
451 then further applied by many others (e.g. Huang et al., 2006; Rossi et al., 2009; Wang et al.,  
452 2009), if this ratio is lower than 25% the spatial dependence is considered strong; if the ratio  
453 is between 25-75% the dependence is considered moderate; and if this ratio is higher than  
454 75% the dependence is considered weak. A similar approach was used here, but their

455 moderate range of spatial dependence (25-75%), that in our opinion is quite wide, was  
456 subdivided, and the following classes of spatial dependency used: class I (very strong) <25%,  
457 class II (moderately strong) = 25-50%, class III (moderately weak) = 50-75%, class IIII (very  
458 weak) >75%, and class O (null) = 100%. Hence, spatial dependence of evaluated soil  
459 properties was mostly moderately strong to very strong in the new resettlement area;  
460 moderately weak to moderately strong in the old resettlement area; and null to moderately  
461 weak in the communal area (Figure 7, Table 3). In fact, in the communal area N and CEC  
462 showed null spatial dependency, while sand, clay and Mg exhibited a linear trend with an  
463 undefined spatial autocorrelation at the considered lag distance. From the other two areas  
464 only N in the old resettlement area exhibited lack of spatial dependence. All the rest of the  
465 cases could be very well represented by spherical models with variable parameters depending  
466 on the soil property and area under evaluation. For example, while the nugget-to-sill ratio for  
467 Ca was 74% in the communal area (moderately weak dependency), in the old and new  
468 resettlement areas this ratio reduced to 42 and 28% (moderately strong dependency),  
469 respectively. This contrasted with silt, as the nugget-to-sill ratio increased from 30 and 34%  
470 in the communal and old resettlement area, respectively, up to 67% in the new resettlement  
471 area. Ranges of the semivariograms for all soil properties and sites ranged from 250 m (silt in  
472 the communal area) to 695 m (clay in the new resettlement). With the exception of Ca,  
473 estimated ranges were lowest in the communal area and highest in the new resettlement.

474

### 475 *3.5. Principal components and geo-statistical analyses of MIRS data*

476 Forty nine percent (49%) of overall variability of MIRS data could be explained by the first  
477 principal component (PC1), while 11, 10, 6, 4 and 4% could be explained by PC2, PC3, PC4,  
478 PC5 and PC6 respectively. Therefore, only the first three components, accounting for 70% of  
479 overall variability, were retained. Scores of the first three components were next correlated to

480 concentration values of reference samples. In general, PC1 related very well to texture  
481 fractions, C, N, Ca and Mg (absolute Spearman coefficient values of 0.55-0.96, Figure 8);  
482 while relationships between PC2 or PC3 with analyzed soil properties were weaker (0.39-  
483 0.69) or mostly non significant (0.01-0.27), respectively (data not shown).

484

485 Standardized semivariograms based on the principal components were usually represented  
486 very well by spherical models, with variable parameters according to the component and  
487 village. PC1, however, showed a linear trend in the communal area, indicating an undefined  
488 spatial dependence at the considered lag distance. In fact, semivariograms showed mainly  
489 that spatial dependence was usually moderately strong to very strong in the new resettlement  
490 area; moderate weak to moderately strong in the old resettlement area; and very weak to  
491 moderately weak in the communal area (Figure 9, Table 4). Ranges of these semivariograms  
492 were 399 m (in the communal area), 161-481 m in the old resettlement area, and 604-744 m  
493 in the new resettlement.

494

#### 495 **4. Discussion**

##### 496 *4.1. MIRS and Geostatistics: a viable combination?*

497 This study clearly illustrated that MIRS can be successfully used for complementing large  
498 soil datasets required for spatial assessments at landscape level. Furthermore, it suggested  
499 that spectral information from MIRS, after principal component analyses, could be directly  
500 integrated in geostatistical analyses without the need of a calibration/validation step.  
501 Effectively, MIRS proved its potential in predicting most of the soil properties under  
502 evaluation; although the technique was not effective for all properties. This was evident for  
503 silt,  $P_{av}$ , K and Al which presented inadequate MIRS models and therefore, predictions for  
504 these variables could not be carried out. Hence, semivariograms for silt,  $P_{av}$ , K and Al were

505 not constructed due to insufficient data. Working with different soils in Vietnam, and by  
506 using the same MIRS methodology and equipment, Schmitter et al. (2010) found, conversely,  
507 acceptable models for silt and K; while their models for clay and CEC were inadequate (P.  
508 Schmitter, personal communication). Hence, applicability and efficacy of MIRS depends on  
509 the soil type and/or location, and illustrates why regional calibrations are still required for a  
510 successful prediction of soil properties (McBratney et al., 2006; Shepherd and Walsh, 2004).  
511 These issues limit a generic applicability of MIRS in the prediction of soil variables for agro-  
512 ecological assessments. Some advances in the development of global calibrations, however,  
513 have been achieved in the last few years (Brown et al., 2005; Cécillon et al., 2009), which  
514 should help to overcome this limitation in the near future. Alternative solutions could be the  
515 use of MIRS-based predictions models to estimate through pedotransfer functions those soil  
516 properties that cannot be predicted accurately by sole MIRS (McBratney et al., 2006), or the  
517 utilization of auxiliary predictors (i.e. simple and inexpensive conventional soil parameters,  
518 like pH and sand; or from complementary sensors, like NIRS) that can improve the prediction  
519 of other soil properties (Brown et al., 2005). Thus, all data could be later used in spatial  
520 analyses without restriction.

521

522 Semivariograms based on the soil dataset clearly showed that spatial autocorrelation of most  
523 soil properties in the villages followed the order: communal area < old resettlement < new  
524 resettlement. Variography analyses based on the principal components from MIRS data  
525 showed comparable spatial patterns (i.e., nugget to sill ratios and ranges of semivariograms,  
526 Figure 10). This implies important savings in terms of analytical costs and time, as it creates  
527 the possibility of a broad and quick assessment of soil spatial variability at landscape scale  
528 based only on MIRS, confirming previous suggestions by Shepherd and Walsh (2007) and  
529 complementing studies based on NIRS (i.e. by Awiti et al., 2008; Cohen et al., 2006; Vågen

530 et al., 2006). A related approach to our study, but at plot level and by using NIRS, was  
531 carried out by Odlare et al. (2005). However, they found out that spatial dependence from  
532 principal components (based on spectral information) was not related to the spatial  
533 dependence from considered soil properties (i.e. C, clay and pH). Hence, although spatial  
534 variation based on NIRS could be identified, the authors did not know what the variation  
535 represented. Thus, to properly understand the meaning of the spatial structures from the  
536 principal components it is necessary to link the component scores to soil parameters of  
537 reference samples. In our case, this was possible for the first principal component (PC1),  
538 which was well related to textural fractions, C, N, Ca, Mg and CEC. Therefore, PC1 was  
539 clearly associated to soil fertility, and thus, derived spatial results could be used for  
540 distinguishing areas of different soil quality. However, for PC2 and PC3 simple relationships  
541 with measured variables were not evident. A reason for this may be related to the explained  
542 variance in each component, where PC1 accounted for 49% of the overall variability, while  
543 the other two components each explained a lower proportion (10-11%). The unexplained  
544 variance and lack of relationships for the other components would indicate that MIRS could  
545 be either generating noise or capturing additional characteristics of soils that this study did  
546 not take into account (e.g. carbonates, lime requirements, dissolved organic C, phosphatase  
547 and urease activity, among others). In fact, MIRS can be related to a wide range of physical,  
548 chemical and biological soil characteristics (for further details please refer to Shepherd and  
549 Walsh, 2007; and Viscarra-Rossel et al., 2006). All this would further suggest that MIRS may  
550 present great potential as an integrative measurement of soil status and, hence, could be a  
551 valuable tool for characterizing spatial variation of soils.

552

553 *4.2 Analyses of spatial patterns*

554 Nearly all experimental semivariograms of soil properties were very well described by the  
555 spherical model, with a reachable sill, which clearly indicates the presence of spatial  
556 autocorrelation. However, some of the semivariograms in the communal area (for sand, clay,  
557 Mg and PC1), could only be described by a linear model with an undefined spatial  
558 dependence. If there is no reachable sill this could indicate that spatial dependence may exist  
559 beyond the considered lag distance (Huang et al., 2006). Semivariograms for N and CEC in  
560 the communal area, and N in the old resettlement showed instead pure nugget effect. Pure  
561 nugget effect can represent either extreme homogeneity (all points have similar values) or  
562 extreme heterogeneity (values are very different, in a random way). However, pure nugget  
563 effect do not compulsory reveal spatial independence, as spatial structure may be present but  
564 at lower resolution than our minimum sample distance (that in our case was 30 m) (Davidson  
565 and Csillag, 2003). In any case, a high nugget effect would imply higher uncertainty when  
566 further interpolation is necessary (e.g. by using Kriging). In such circumstances, calculating  
567 the mean value from sampled locations would be sufficient for interpolation, as no spatial  
568 structure could be detected at the scale of observation. Finding no spatial dependence for  
569 some soil parameters is not an unusual result, as its magnitude (from strong to null  
570 dependency) can vary as a function of the soil property and location, among others factors  
571 (Garten Jr. et al., 2007).

572

573 As indicated before, spatial dependence (either based on soil properties or just on MIR  
574 spectral data) was in general lowest in the communal area and highest in the new  
575 resettlement. Although the reasons for these differences can not be completely determined,  
576 since our experimental design did not allow a proper separation of causal factors, direct and  
577 indirect evidence would suggest some potential drivers that nevertheless need to be  
578 investigated in future studies. For example, it is generally accepted (Cambardella et al., 1994;



579 Liu et al., 2004; Liu et al., 2009; R uth and Lennartz, 2008) that a strong spatial dependency  
580 of soil properties is controlled by intrinsic factors, like texture and mineralogy; while a weak  
581 dependence is attributed to extrinsic factors, like farmers' management (e.g. fertilizer  
582 applications). Thus, in terms of intrinsic factors, spatial dependence seems to follow the  
583 particular textural classes and inherent soil quality of each area. In terms of extrinsic factors,  
584 findings from Cobo et al. (2009) would support this as investment in soil fertility and land  
585 management of cropping fields was higher in the communal area than in the two resettlement  
586 areas. Moreover, according to the history of each settlement (Cobo et al., 2009) the grade of  
587 disturbance of natural resources is in the order: communal area > old resettlement > new  
588 resettlement, which would also affect correspondingly the spatial variability of soil  
589 properties. The coefficient of variation of evaluated soil properties seems to support this, as  
590 (with the exception of pH and sand) usually the highest CVs were obtained in the communal  
591 area, while the lowest values were found in the new resettlement. However, despite this  
592 global trend, no clear relationships were found between the CVs and their respective spatial  
593 variability parameters, which indicates once more that only part of the variation could be  
594 explained. Similar observations between CVs and spatial variability parameters have been  
595 also reported by Gallardo and Param a (2007).

596

#### 597 *4.3. Relevance of findings for future sampling designs*

598 Knowledge of sample sizes for each soil property and village presented in this study could be  
599 used as guide for better planning sampling designs at landscape scale in areas of similar  
600 conditions, as it helps to estimate approximate minimum number of samples that must be  
601 taken in each location for achieving a predetermined level of precision. These data, however,  
602 do not indicate how samples should be distributed in space. Derived ranges from variography  
603 analyses complement very well this information. They indicate the adequate sample distances

604 among points for obtaining spatially-independent samples (i.e. that distance that exceeds the  
605 ranges of the semivariograms), as better results are obtained when samples are not  
606 autocorrelated (Rossi et al., 2009). However, when a high level of precision is required,  
607 collection of spatially-independent samples may be problematic, especially for those  
608 properties exhibiting high ranges, due to the potential difficulty of arranging a high number  
609 of samples at the required (i.e. long) separation distances. For example, for C assessments, if  
610 a 5% of error is selected, a minimum of 264 samples should be distributed at >577 m of  
611 separation among each other in the new resettlement, which is simply not possible if we  
612 consider the same spatial domain. However, at 10% of error, only 66 samples are needed,  
613 thus their distribution in the same area is feasible. In the case of sand, clay, N, Mg and CEC  
614 for the communal area, and N for the old resettlement, samples could be placed at random  
615 instead, as these properties showed pure nugget effect. Data for pH, on the other hand, should  
616 be cautiously interpreted, as it is already in a logarithmic scale; hence, not surprisingly it  
617 showed the lowest CVs and minimum sample sizes. If the intention of the sampling is to  
618 characterize again the spatial variability within villages, results indicated that a sampling  
619 distance of 30 m is acceptable for the new resettlement; but lower distances may be necessary  
620 for the communal and old resettlement to be able to capture shorter-range variability which  
621 this study was not be able to detect. In any case, care is required if direct extrapolation of  
622 sampling sizes and ranges to other scales is carried out (e.g. at plot or national levels), as  
623 spatial dependence usually differ with the scale (Cambardella et al., 1994).

624

## 625 **5. Conclusions**

626 Results from this study clearly showed that required large soil datasets can be built by using  
627 MIRS for the prediction of several soil properties, and later successfully used in geostatistical  
628 analyses. However, it was also illustrated that not all soil properties exhibit a MIR spectral

629 response, and those ones who were well predicted (i.e. sand, clay, pH, C, N, Ca, Mg and  
630 CEC) usually depend on the success of regional calibrations. As a new approach, results  
631 showed that MIRS data could be directly integrated, after principal component analyses, in  
632 geostatistic assessments without the necessity of calibration/validation steps. This approach is  
633 very useful when time and funds are limited, and when a coarse measure of soil spatial  
634 variability is required. However, principal components must be associated to soil functional  
635 characteristics to be able to explain the results, as was demonstrated with the soil properties  
636 considered in this study. Understanding variability of soils and its spatial patterns in these  
637 three contrasting areas brought out also important recommendations for future sampling  
638 designs and mapping. By combining information about minimum sample sizes, with  
639 corresponding reported ranges from the semivariograms, a better efficiency (in terms of time,  
640 costs and accuracy) during sampling exercises could be obtained. Hence, it is concluded that  
641 MIRS and geostatistics can be successfully integrated for spatial landscape analyses and  
642 monitoring. A similar approach would be very valuable in regional and global soil fertility  
643 assessments and mapping (e.g. Sanchez et al., 2009) and carbon sequestration campaigns  
644 (e.g. Goidts et al., 2009), where large soil sample sizes are required and uncertainty about  
645 sampling designs prevail.

646

## 647 **6. Acknowledgments**

648 The authors are grateful to all farmers in the three villages who supported this study. Many  
649 thanks also go to: the extension officers in the region for their collaboration; to Stefan  
650 Becker, Cheryl Batistel and the staff of Landesanstalt für Landwirtschaftliche Chemie in the  
651 University of Hohenheim for laboratory analyses; to Irene Chukwumah for her support  
652 during MIRS readings; and to Hans-Peter Piepho for assistance during statistical analyses.  
653 Thanks also to Andrea Schmidt (Bruker Optik GmbH) for her useful help during the analyses

654 of MIRS data. The methodology development of this study is linked to the DFG-funded  
655 project PAK 346 (“Structure and functions of agricultural landscapes under global climate  
656 change”), subproject P3.

657

## 658 **7. References**

- 659 Anderson, J.M. and Ingram, J.S.I., 1993. *Tropical Soil Biology and Fertility: A Handbook of*  
660 *Methods*. CAB International, Wallingford, Oxon, 221 pp.
- 661 Awiti, A.O., Walsh, M.G., Shepherd, K.D. and Kinyamario, J., 2008. Soil condition  
662 classification using infrared spectroscopy: A proposition for assessment of soil  
663 condition along a tropical forest-cropland chronosequence. *Geoderma*, 143: 73-84.
- 664 Bekele, A. and Hudnall, W.H., 2006. Spatial variability of soil chemical properties of a  
665 prairie-forest transition in Louisiana. *Plant and Soil*, 280: 7-21.
- 666 Borůvka, L., Mládková, L., Penížek, V., Drábek, O. and Vašát, R., 2007. Forest soil  
667 acidification assessment using principal component analysis and geostatistics.  
668 *Geoderma*, 140: 374-382.
- 669 Bray, R.H. and Kurtz, L.T., 1945. Determination of total, organic, and available forms of  
670 phosphorus in soils. *Soil Science*, 59: 39-45.
- 671 Brown, D.J., Shepherd, K.D., Walsh, M.G., Mays, M.D. and Reinsch, T.G., 2005. Global soil  
672 characterization with VNIR diffuse reflectance spectroscopy. *Geoderma*, 132(3-4):  
673 273-290.
- 674 Cambardella, C.A., Moorman, T.B., Novak, J.M., Parkin, T.B., Karlen, D.L., Turco, R.F. and  
675 Konopka, A.E., 1994. Field-Scale Variability of Soil Properties in Central Iowa Soils.  
676 *Soil Science Society of America Journal*, 58: 1501-1511.
- 677 Cécillon, L., Barthès, B.G., Gomez, C., Ertlen, D., Genot, V., Hedde, M., Stevens, A. and  
678 Brun, J.J., 2009. Assessment and monitoring of soil quality using near-infrared  
679 reflectance spectroscopy (NIRS). *European Journal of Soil Science*, 60: 770-784.
- 680 Cobo, J.G., Dercon, G. and Cadisch, G., 2010. Nutrient balances in African land use systems  
681 across different spatial scales: a review of approaches, challenges and progress.  
682 *Agriculture, Ecosystem and Environment*, 136(1-2): 1-15.
- 683 Cobo, J.G., Dercon, G., Monje, C., Mahembe, P., Gotosa, T., Nyamangara, J., Delve, R. and  
684 Cadisch, G., 2009. Cropping strategies, soil fertility investment and land management  
685 practices by smallholder farmers in communal and resettlement areas in Zimbabwe.  
686 *Land Degradation & Development*, 20(5): 492-508.
- 687 Cohen, M., Dabral, S., Graham, W., Prenger, J. and Debusk, W., 2006. Evaluating Ecological  
688 Condition Using Soil Biogeochemical Parameters and Near Infrared Reflectance  
689 Spectra. *Environmental Monitoring and Assessment*, 116: 427-457.
- 690 Conzen, J.-P., 2003. *Multivariate Calibration: A Practical Guide for the Method Development*  
691 *in the Analytical Chemistry*. Bruker Optik GmbH, 92 pp.
- 692 Davidson, A. and Csillag, F., 2003. A comparison of nested analysis of variance (ANOVA)  
693 and variograms for characterizing grassland spatial structure under a limited sampling  
694 budget. *Canadian Journal of Remote Sensing*, 29: 43-56.
- 695 Dercon, G., Deckers, J., Govers, G., Poesen, J., Sanchez, H., Vanegas, R., Ramirez, M. and  
696 Loai, G., 2003. Spatial variability in soil properties on slow-forming terraces in the  
697 Andes region of Ecuador. *Soil and Tillage Research*, 72: 31-41.

- 698 FAO, 2005. Land Cover Classification System. Classification concepts and user manual,  
699 Software version 2. Environment and natural resources series 8. FAO, Rome, Italy.
- 700 Fortin, M.-J., Dale, M.R.T. and Hoef, J.v., 2002. Spatial analysis in ecology. In: A.H. El-  
701 Shaarawi and W.W. Piegorsch (Editors), *Encyclopedia of Environmetrics*. John Wiley  
702 & Sons, Ltd, Chichester, pp. 2051-2058.
- 703 Gallardo, A. and Paramá, R., 2007. Spatial variability of soil elements in two plant  
704 communities of NW Spain. *Geoderma*, 139: 199-208.
- 705 Garten Jr., C.T., Kanga, S., Bricea, D.J., Schadta, C.W. and Zho, J., 2007. Variability in soil  
706 properties at different spatial scales (1 m–1 km) in a deciduous forest ecosystem. *Soil  
707 Biology & Biochemistry*, 39: 2621-2627.
- 708 Giller, K.E., Rowe, E.C., De Ridder, N. and Van Keulen, H., 2006. Resource use dynamics  
709 and interactions in the tropics: Scaling up in space and time. *Agricultural Systems*, 88:  
710 8-27.
- 711 Goidts, E., Wesemael, B.V. and Crucifix, M., 2009. Magnitude and sources of uncertainties  
712 in soil organic carbon (SOC) stock assessments at various scales. *European Journal of  
713 Soil Science*, 60: 723-739.
- 714 Goovaerts, P., 1999. Geostatistics in soil science: state-of-the-art and perspectives.  
715 *Geoderma*, 89: 1-45.
- 716 Huang, S.-W., Jin, J.-Y., Yang, L.-P. and Bai, Y.-L., 2006. Spatial variability of soil nutrients  
717 and influencing factors in a vegetable production area of Hebei Province in China.  
718 *Nutrient Cycling in Agroecosystems*, 75: 201-212.
- 719 Janik, L.J., Merry, R.H. and Skjemstad, J.O., 1998. Can mid infrared diffuse reflectance  
720 analysis replace soil extractions? *Australian Journal of Experimental Agriculture*, 38:  
721 681-196.
- 722 Liebhold, A.M. and Gurevitch, J., 2002. Integrating the statistical analysis of spatial data in  
723 ecology. *Ecography*, 25: 553–557.
- 724 Lin, H., Wheeler, D., Bell, J. and Wilding, L., 2005. Assessment of soil spatial variability at  
725 multiple scales. *Ecological Modelling*, 182: 271-272.
- 726 Liu, X., Xu, J., Zhang, M. and Zhou, B., 2004. Effects of Land Management Change on  
727 Spatial Variability of Organic Matter and Nutrients in Paddy Field: A Case Study of  
728 Pinghu, China. *Environmental Management*, 34: 691-700.
- 729 Liu, X., Zhang, W., Zhang, M., Ficklin, D.L. and Wang, F., 2009. Spatio-temporal variations  
730 of soil nutrients influenced by an altered land tenure system in China. *Geoderma*, 152:  
731 23-34.
- 732 Makkawi, M.H., 2004. Integrating GPR and geostatistical techniques to map the spatial  
733 extent of a shallow groundwater system. *Journal of Geophysics and Engineering*, 1:  
734 56-62.
- 735 McBratney, A.B., Minasny, B. and Rossel, R.V., 2006. Spectral soil analysis and inference  
736 systems: A powerful combination for solving the soil data crisis. *Geoderma*, 136: 272-  
737 278.
- 738 Odlare, M., Svensson, K. and Pell, M., 2005. Near infrared reflectance spectroscopy for  
739 assessment of spatial soil variation in an agricultural field. *Geoderma*, 126: 193-202.
- 740 Olea, R.A., 2006. A six-step practical approach to semivariogram modeling. *Stochastic  
741 Environmental Research and Risk Assessment*, 20: 307-318.
- 742 Pirie, A., Singh, B. and Islam, K., 2005. Ultra-violet, visible, near-infrared, and mid-infrared  
743 diffuse reflectance spectroscopic techniques to predict several soil properties.  
744 *Australian journal of soil research*, 43: 713-721.
- 745 Pozdnyakova, L., Gimenez, D. and Oudemans, P.V., 2005. Spatial Analysis of Cranberry  
746 Yield at Three Scales. *Agronomy Journal*, 97: 49-57.

- 747 Reimann, C. and Filzmoser, P., 2000. Normal and lognormal data distribution in  
748 geochemistry : death of a myth. Consequences for the statistical treatment of  
749 geochemical and environmental data. *Environmental geology*, 39: 1001-1014.
- 750 Rossi, J., Govaerts, A., Vos, B.D., Verbist, B., Vervoort, A., Poesen, J., Muys, B. and  
751 Deckers, J., 2009. Spatial structures of soil organic carbon in tropical forests - A case  
752 study of Southeastern Tanzania. *Catena*, 77: 19-27.
- 753 R  th, B. and Lennartz, B., 2008. Spatial Variability of Soil Properties and Rice Yield Along  
754 Two Catenas in Southeast China. *Pedosphere*, 18: 409-420.
- 755 Samake, O., Smaling, E.M.A., Kropff, M.J., Stomph, T.J. and Kodio, A., 2005. Effects of  
756 cultivation practices on spatial variation of soil fertility and millet yields in the Sahel  
757 of Mali. *Agriculture, Ecosystems and Environment* 109: 335-345.
- 758 Sanchez, P.A. et al., 2009. Digital Soil Map of the World. *Science*, 325: 680-681.
- 759 Sanchez, P.A. and Leakey, R.R.B., 1997. Land use transformation in Africa: three  
760 determinants for balancing food security with natural resource utilization. *European*  
761 *Journal of Agronomy*, 7: 15-23.
- 762 Sauer, T.J., Cambardella, C.A. and Meek, D.W., 2006. Spatial variation of soil properties  
763 relating to vegetation changes. *Plant and Soil*, 280: 1-5.
- 764 Schmitter, P., Dercon, G., Hilger, T., Le Ha, T., Thanh, N.H., Vien, T.D., Lam, N.T. and  
765 Cadisch, G., 2010. Sediment induced soil spatial variation in paddy fields of  
766 Northwest Vietnam. *Geoderma*, 155(3-4): 298-307.
- 767 Sch  ning, A. and Br  mmer, G.W., 2008. Extraction of mobile element fractions in forest  
768 soils using ammonium nitrate and ammonium chloride. *Journal of Plant Nutrition and*  
769 *Soil Science* 171: 392-398.
- 770 Shepherd, K.D. and Walsh, M.G., 2004. Diffuse Reflectance Spectroscopy for Rapid Soil  
771 Analysis. In: R. Lal (Editor), *Encyclopedia of Soil Science*. Marcel Dekker, Inc.
- 772 Shepherd, K.D. and Walsh, M.G., 2007. Infrared spectroscopy - enabling an evidence-based  
773 diagnostic surveillance approach to agricultural and environmental management in  
774 developing countries. *Journal of Near Infrared Spectroscopy*, 15: 1-20.
- 775 Urban, D.L., 2002. Tactical monitoring of landscapes. In: J. Liu and W.W. Taylor (Editors),  
776 *Integrating Landscape Ecology into Natural Resource Management*. Cambridge  
777 University Press, Cambridge, pp. 294-311.
- 778 V  gen, T.-G., Shepherd, K.D. and Walsh, M.G., 2006. Sensing landscape level change in soil  
779 fertility following deforestation and conversion in the highlands of Madagascar using  
780 Vis-NIR spectroscopy. *Geoderma*, 133: 281-294.
- 781 Viscarra-Rossel, R.A., T, D.J.J.W., McBratney, A.B., Janik, L.J. and Skjemstad, J.O., 2006.  
782 Visible, near infrared, mid infrared or combined diffuse reflectance spectroscopy for  
783 simultaneous assessment of various soil properties. *Geoderma*, 131: 59-75.
- 784 Vitousek, P.M. et al., 2009. Nutrient Imbalances in Agricultural Development. *Science*, 324:  
785 1519-1520.
- 786 Wang, Y., Zhang, X. and Huang, C., 2009. Spatial variability of soil total nitrogen and soil  
787 total phosphorus under different land uses in a small watershed on the Loess Plateau,  
788 China. *Geoderma*, 150: 141-149.
- 789 Wei, J.-B., Xiao, D.-N., Zeng, H. and Fu, Y.-K., 2008. Spatial variability of soil properties in  
790 relation to land use and topography in a typical small watershed of the black soil  
791 region, northeastern China. *Environmental Geology*, 53: 1663-1672.
- 792 Yan, X. and Cai, Z., 2008. Number of soil profiles needed to give a reliable overall estimate  
793 of soil organic carbon storage using profile carbon density data. *Soil Science and*  
794 *Plant Nutrition*, 54: 819-825.

795 Yemefack, M., Rossiter, D.G. and Njomgang, R., 2005. Multi-scale characterization of soil  
796 variability within an agricultural landscape mosaic system in southern Cameroon.  
797 *Geoderma*, 125: 117-143.  
798  
799

800 Table 1. Main characteristics of the villages under study

801

Village name	Settlement type	Settlement time	Location (District, Ward)	Dominant soil type <sup>&amp;</sup>	Mean soil textural class	Village area (ha)
Kanyera	Communal area	1948	Shamva, 6	Chromic Luvisols	Loamy sand	730
Chomutomora	Old resettlement	1987	Shamva, 15	Chromic Luvisols	Sandy Loam	780
Hereford Farm	New resettlement	2002	Bindura, 8	Rhodic Ferrasols	Clay	1360

802

803 <sup>&</sup> According to FAO soil classification



804 Table 2. Optimization parameters and performance indicators of best MIRS models for each soil property under evaluation.

805

Property	n	Outliers removed	Preprocessing method <sup>&amp;</sup>	Rank	Calibration			Validation			Prediction
					$R^2$	RMSEE	RPD	$R^2$	RMSEP	RPD	
Sand	110	1	1stDer+VN	7	0.98	3.7	6.7	0.98	3.3	6.8	Yes
Silt	110	1	1stDer+VN	6	0.85	3.1	2.6	0.82	3.6	2.4	No <sup>#</sup>
Clay	110	1	1stDer+SLS	3	0.97	3.0	6.1	0.97	2.6	6.2	Yes
pH	165	2	1stDer+SLS	9	0.93	0.20	3.8	0.89	0.24	3.1	Yes
C	165	1	1stDer+VN	14	0.99	0.14	10.1	0.98	0.19	6.4	Yes
N	165	2	1stDer+VN	9	0.98	0.01	6.6	0.96	0.02	5.2	Yes
P <sub>av</sub>	165	0	SLS	6	0.47	5.5	1.4	0.49	6.2	1.4	No
K	165	0	None	5	0.48	1.9	1.4	0.56	1.4	1.5	No
Ca	165	1	COE	8	0.94	25.2	4.1	0.96	18.7	5.1	Yes
Mg	165	0	1stDer+MSC	8	0.96	14.8	5.2	0.92	18.0	3.4	Yes
Al	165	0	1stDer+SLS	12	0.69	0.70	1.8	0.66	0.61	1.8	No
CEC	165	0	1stDer+VN	9	0.98	22.8	7.6	0.98	24.4	6.6	Yes

806

807 <sup>&</sup> 1stDer: 1<sup>st</sup> derivative, COE: constant offset elimination, SLS: straight line subtraction, MSC: multiplicative scatter correction, VN: vector  
 808 normalization. Considered spectral regions from the optimization process are not shown.

809 n: number of observations; Rank: number of factors used in the PLS regression; RMSEE: Root Mean Square Error of Estimation, RMSEP:

810 Root Mean Square Error of the Prediction, RPD: Residual Prediction Deviation

811 <sup>#</sup> But could be calculated from the other two textural fractions

812 Table 3. Model parameters of standardized theoretical semivariograms of evaluated soil  
813 properties in the three villages under study. See Figure 7 for a visualization of respective  
814 experimental and theoretical semivariograms.  
815

Property <sup>s</sup>	Outliers removed	Type of Model	$R^2$	$RSS^@$	Nugget $C_0$	Sill $C_0+C$	Range $a$ (in m)	$\frac{C_0}{(C_0+C)}^\#$	Class <sup>&amp;</sup>
<i>Communal area (n=120)</i>									
Sand	0	Linear	0.26	6.79E-00	0.86	1.05	$\infty$	82.1	III
Silt	0	Spherical	0.49	9.35E-01	0.30	1.01	250	29.7	II
Clay <sup>L</sup>	0	Linear	0.25	2.33E-02	0.89	1.09	$\infty$	81.1	III
pH <sup>L</sup>	0	Spherical	0.21	5.64E-04	0.62	0.97	451	63.6	III
C <sup>A</sup>	0	Spherical	0.14	5.53E-05	0.56	1.01	400	56.0	III
N <sup>A</sup>	2	-	-	-	1.0	1.0	$\infty$	100	O
Ca <sup>S</sup>	0	Spherical	0.29	1.08E-02	0.72	0.98	527	73.6	III
Mg <sup>A</sup>	0	Linear	0.25	1.67E-04	0.86	1.04	$\infty$	82.8	III
CEC <sup>L</sup>	0	-	-	-	1.0	1.0	$\infty$	100	O
<i>Old resettlement area (n=132)</i>									
Sand	0	Spherical	0.63	8.58E-00	0.49	0.94	441	51.6	III
Silt <sup>L</sup>	0	Spherical	0.67	5.34E-03	0.36	1.06	426	34.2	II
Clay <sup>L</sup>	0	Spherical	0.59	1.01E-02	0.48	0.95	415	50.4	III
pH <sup>S</sup>	0	Spherical	0.64	1.34E-03	0.51	1.07	484	48.1	II
C <sup>L</sup>	0	Spherical	0.52	7.20E-03	0.69	1.06	532	65.2	III
N <sup>A</sup>	1	-	-	-	1.0	1.0	$\infty$	100	O
Ca <sup>S</sup>	0	Spherical	0.72	3.39E-02	0.45	1.08	483	41.6	II
Mg <sup>A</sup>	0	Spherical	0.56	3.18E-04	0.54	1.09	459	49.8	II
CEC <sup>L</sup>	0	Spherical	0.63	1.31E-02	0.61	1.02	386	60.0	III
<i>New resettlement area (n=180)</i>									
Sand <sup>S</sup>	0	Spherical	0.71	5.11E-02	0.42	1.06	506	39.4	II
Silt	0	Spherical	0.60	8.60E-01	0.69	1.03	671	67.3	III
Clay	0	Spherical	0.76	6.80E-00	0.46	1.05	695	43.7	II
pH <sup>L</sup>	0	Spherical	0.65	1.57E-03	0.39	1.08	638	36.2	II
C <sup>L</sup>	0	Spherical	0.75	1.11E-02	0.23	1.05	577	21.4	I
N <sup>A</sup>	0	Spherical	0.77	6.70E-06	0.23	1.04	517	22.1	I
Ca <sup>S</sup>	0	Spherical	0.64	2.51E-01	0.31	1.10	649	28.1	II
Mg <sup>S</sup>	0	Spherical	0.71	1.98E-01	0.17	1.05	522	15.8	I
CEC <sup>A</sup>	0	Spherical	0.70	4.91E-03	0.25	1.08	604	23.3	I

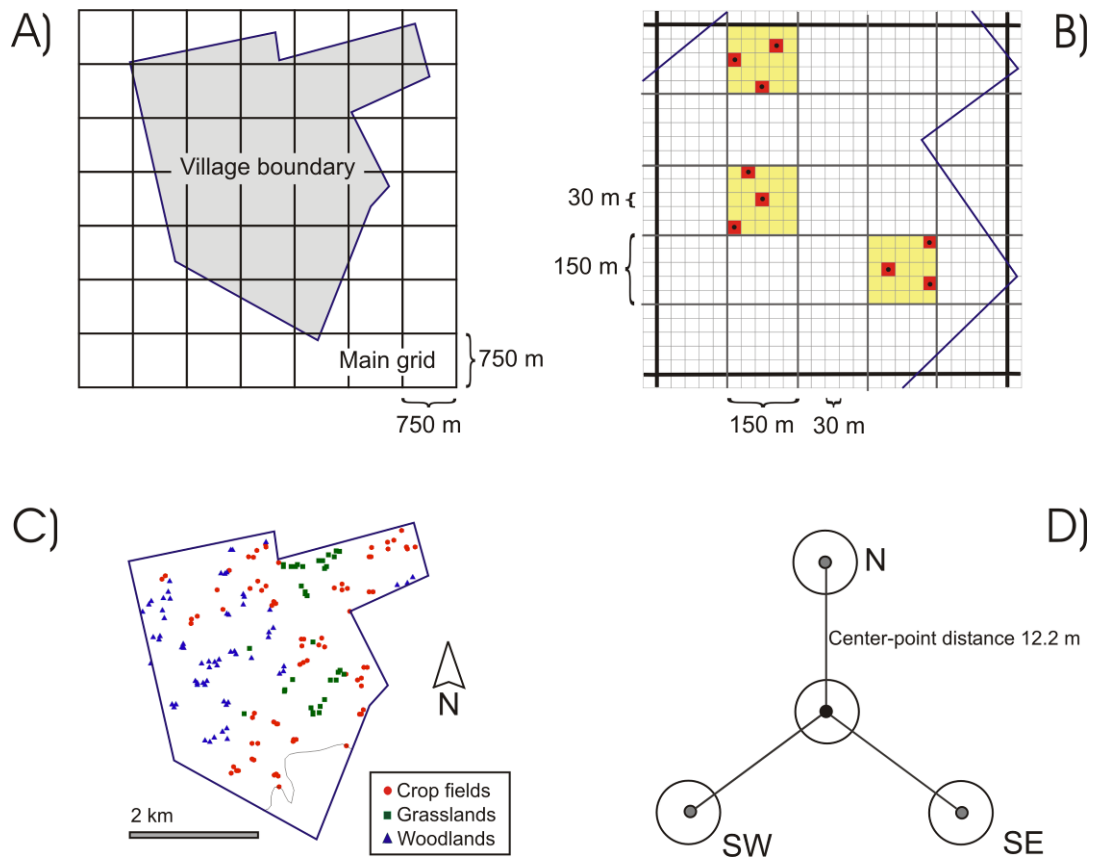
816  
817 <sup>s</sup>: If carried out, the type of transformation is indicated (<sup>L</sup> = logarithm, <sup>S</sup> = square root, <sup>A</sup> =  
818 arcsin, n: number of observations; <sup>@</sup>: Residual Sum of Squares, <sup>#</sup>: Nugget-to-sill ratio (%),  
819 <sup>&</sup>: Spatial dependency class: I = very strong, II = moderately strong, III = moderately weak,  
820 IIII = very weak, O = null.

821

822 Table 4. Model parameters of standardized theoretical semivariograms of the three first  
 823 principal components from MIRS data of the three areas under study. See Figure 8 for a  
 824 visualization of respective experimental and theoretical semivariograms.  
 825

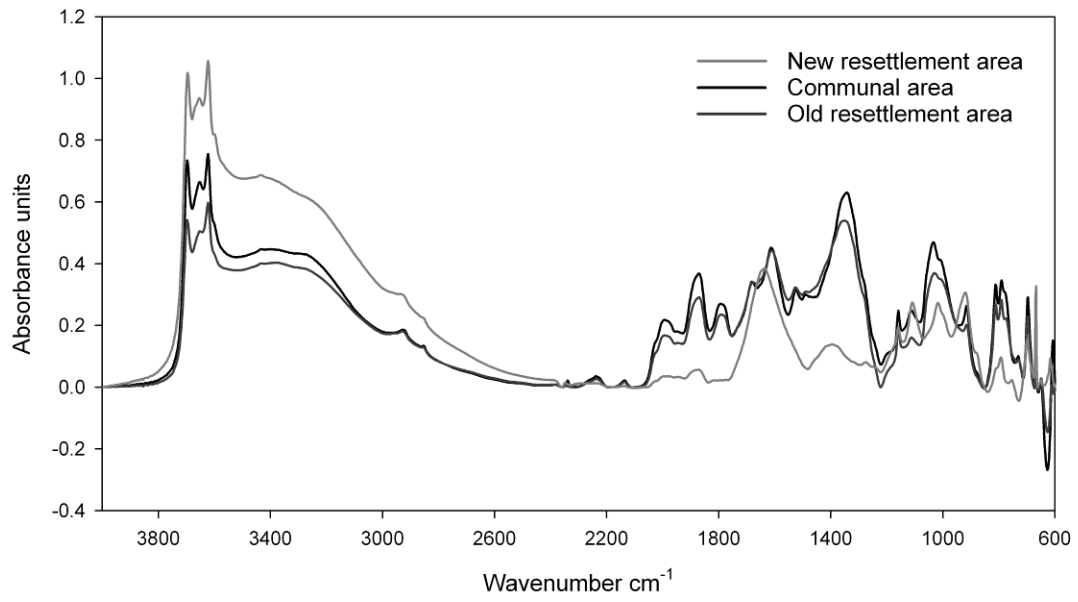
Property <sup>s</sup>	Outliers removed	Type of Model	$R^2$	$RSS^{\textcircled{a}}$	Nugget $C_0$	Sill $C_0+C$	Range $a$ (in m)	$\frac{C_0}{(C_0+C)^{\#}}$	Class <sup>&amp;</sup>
<i>Communal area (n=120)</i>									
PC1 <sup>L</sup>	0	Linear	0.09	4.41E-03	0.94	1.03	$\infty$	90.9	III
PC2	0	Spherical	0.15	3.93E-03	0.59	1.01	399	58.7	III
PC3 <sup>L</sup>	0	Spherical	0.41	6.41E-03	0.60	1.03	399	58.0	III
<i>Old resettlement area (n=132)</i>									
PC1	1	Spherical	0.62	4.44E-03	0.54	1.05	481	51.0	III
PC2 <sup>L</sup>	4	Spherical	0.60	1.60E-03	0.59	1.15	479	51.1	II
PC3 <sup>L</sup>	2	Spherical	0.40	3.73E-03	0.41	0.99	161	41.0	II
<i>New resettlement area (n=180)</i>									
PC1 <sup>A</sup>	1	Spherical	0.69	9.74E-06	0.20	1.10	606	18.3	I
PC2	10	Spherical	0.80	4.66E-05	0.45	1.10	744	41.0	II
PC3	0	Spherical	0.78	2.13E-01	0.05	1.11	604	4.6	I

826  
 827 <sup>s</sup>: If carried out, the type of transformation is indicated (<sup>L</sup> = logarithm, <sup>A</sup> = arcsin), n: number  
 828 of observations; <sup>@</sup>: Residual Sum of Squares, <sup>#</sup>: Nugget-to-sill ratio (%), <sup>&</sup>: Spatial  
 829 dependency class: I = very strong, II = moderately strong, III = moderately weak, IIII = very  
 830 weak.  
 831



832  
833  
834  
835  
836  
837  
838  
839  
840

Figure 1. Soil sampling design. Hereford farm is used here as illustration: A) Representation of the overlay of a village boundary with main grid of 750 x 750 m; B) Zooming into a cell of 750 x 750 m where grids of 150 x 150 and 30 x 30 m, and selected sub-cells and micro-cells (with respective centroids), are shown; C) Final distribution of sampling points in the village; D) Schematic representation of the radial arm for each sampling point, where central circle indicates the centroid of each micro-cell (N: north, SW: south west; SE: south east).



841

842

843

Figure 2. Examples of mid infrared spectra of soil samples from the three villages under

844

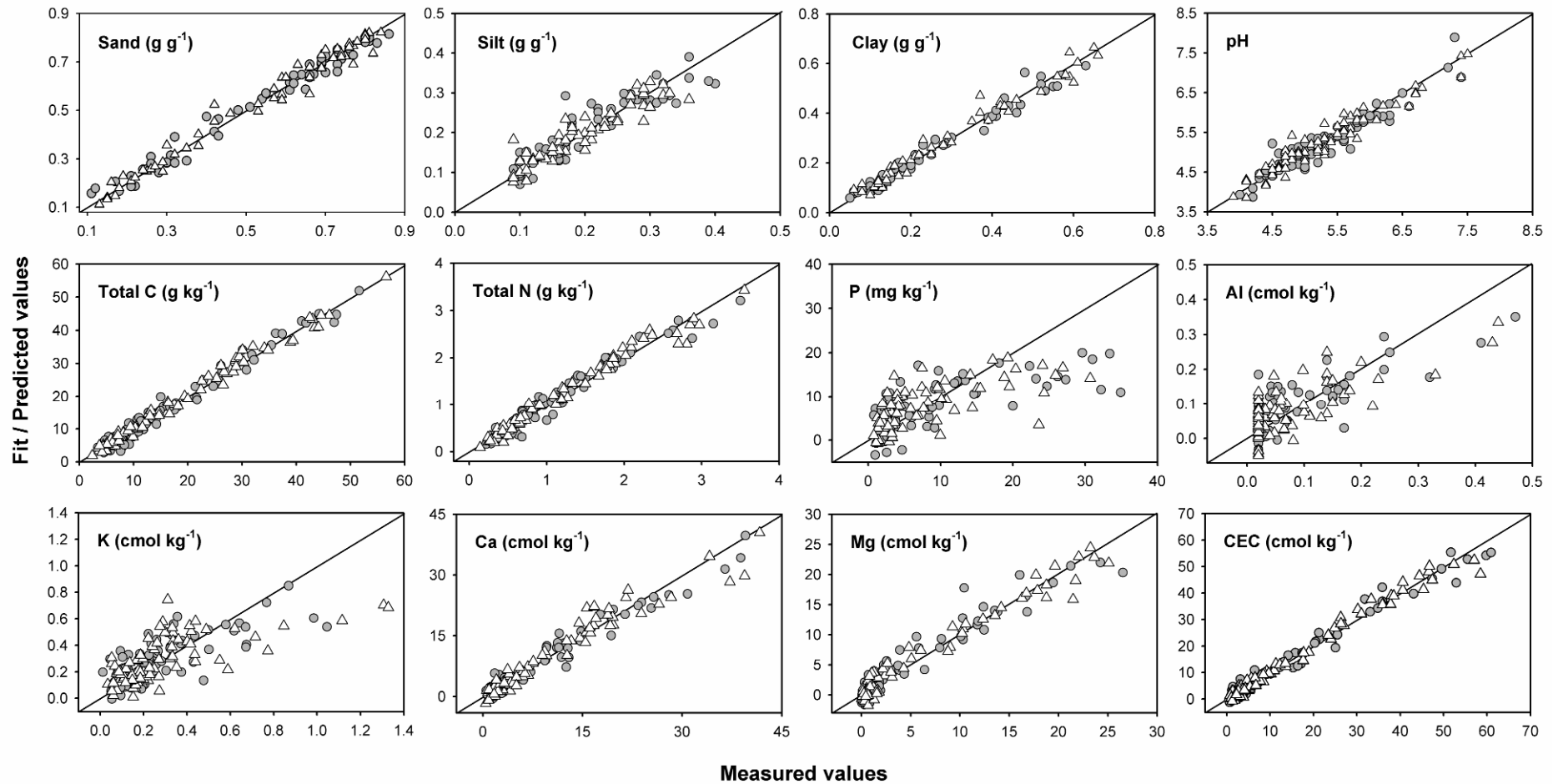
study: i.e. the baseline-corrected spectrum of one sample per village having an average C

845

content of 7, 11 and 29 g kg<sup>-1</sup> for the communal area, and the old and new resettlement areas,

846

respectively.

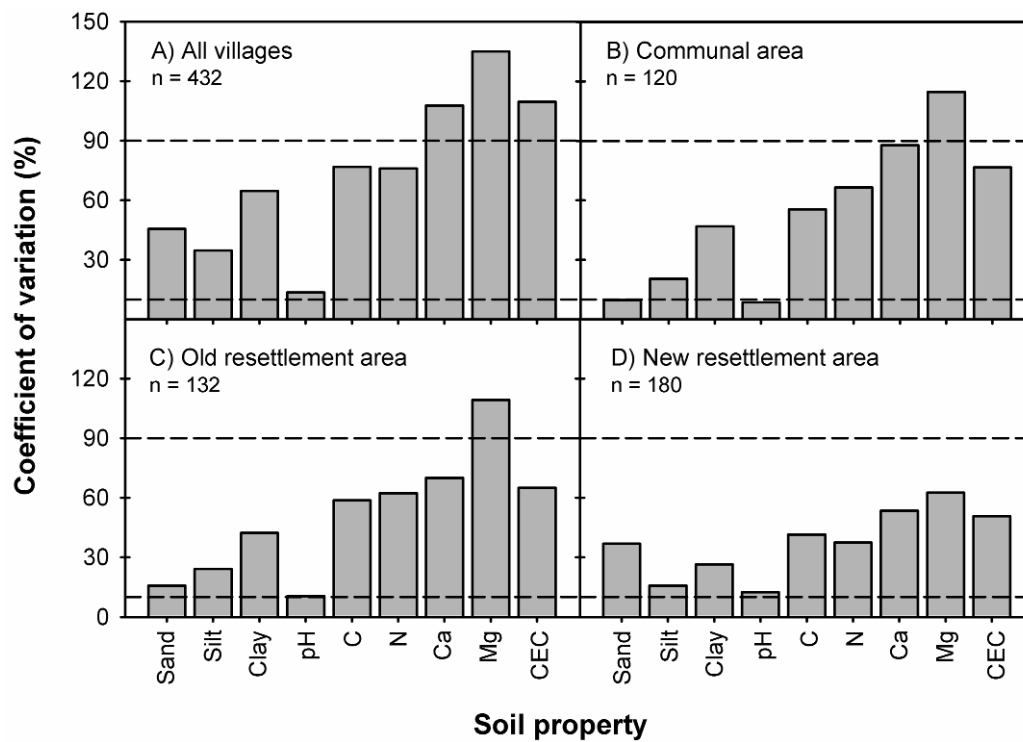


847

848

849 Figure 3. Calibration (triangles) and validation (circles) scatter plots of MIRS models from evaluated soil properties. For respective performance

850 indicators refer to Table 2.



852

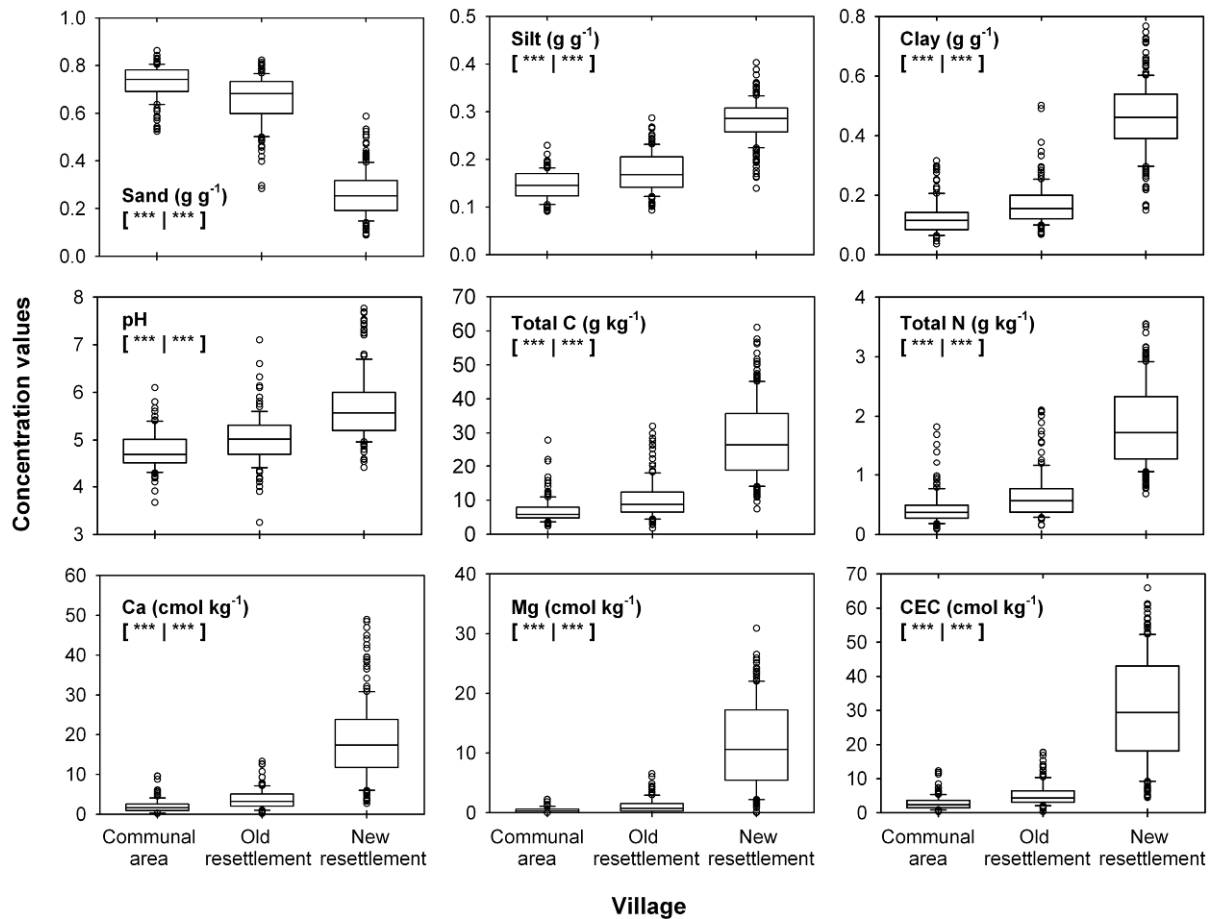
853

854 Figure 4. Coefficient of variation of soil properties in the entire dataset (A), and in each

855 village under evaluation (B-D). Dashed lines indicate reference values of 10 and 90% for low

856 and high variation, respectively.

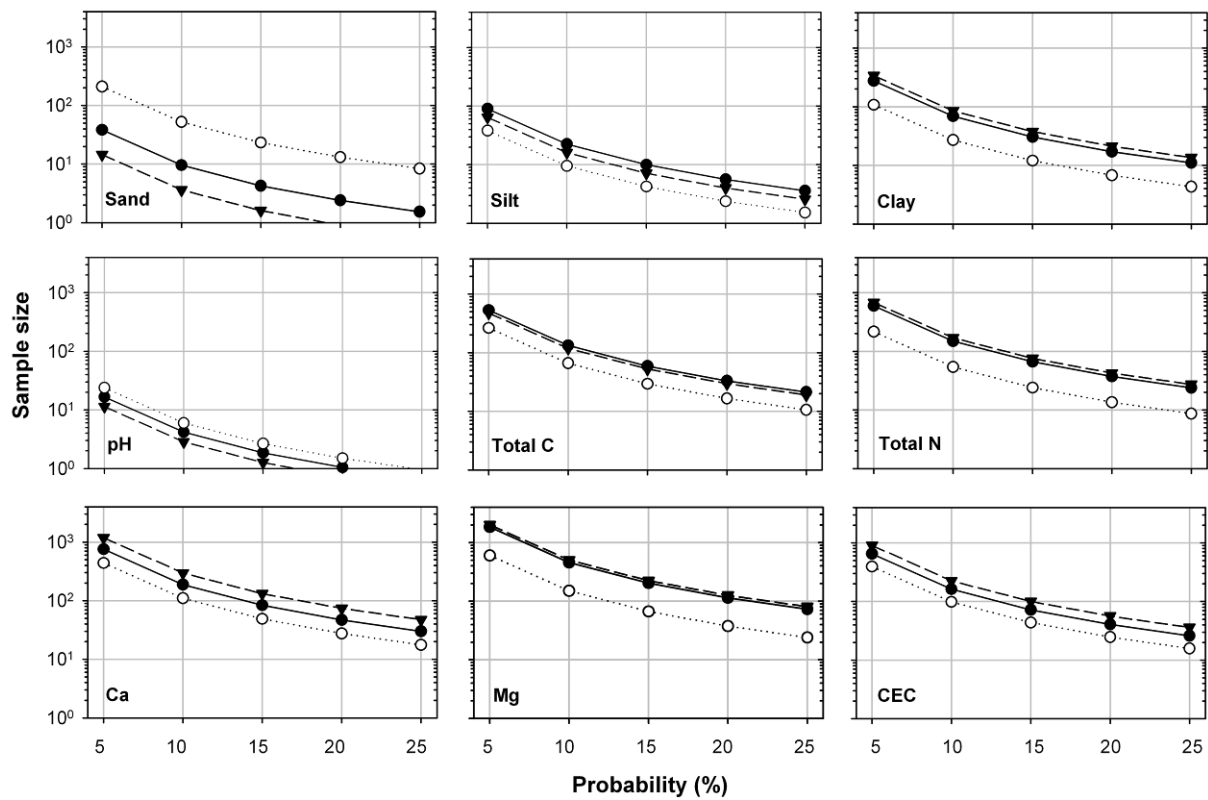
857



858  
 859  
 860  
 861  
 862  
 863  
 864  
 865

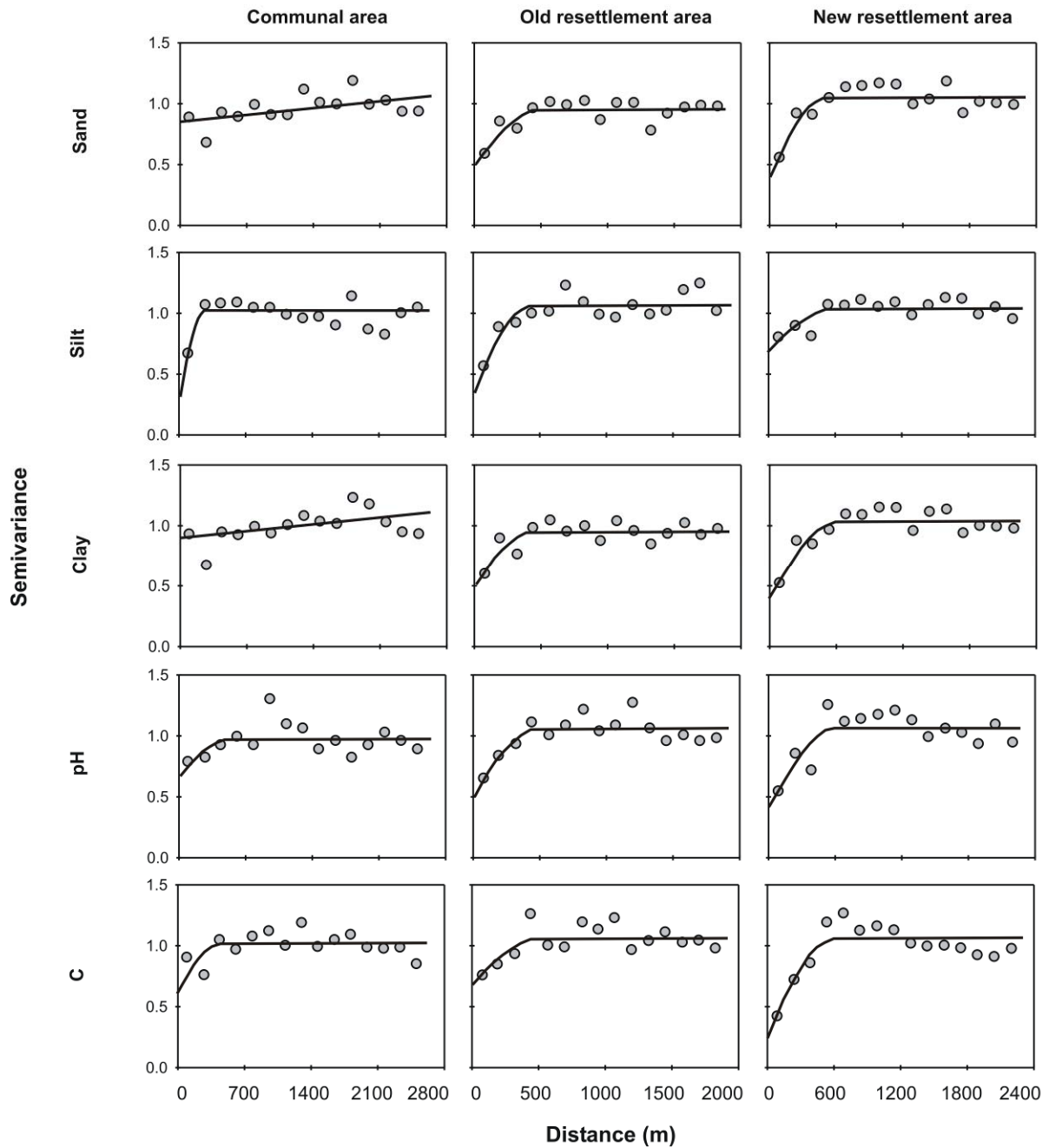
Figure 5. Box and whisker plots of soil properties in each village under evaluation, and associated statistical differences (\*\*\*) :  $p < 0.001$ ) according to the [Kruskall-Wallis | Mann-Whitney] tests. Kruskall-Wallis compared medians (horizontal line inside boxes) of the three villages, while Mann-Whitney compared only the communal and old resettlement areas. Number of data as shown in Figure 4.





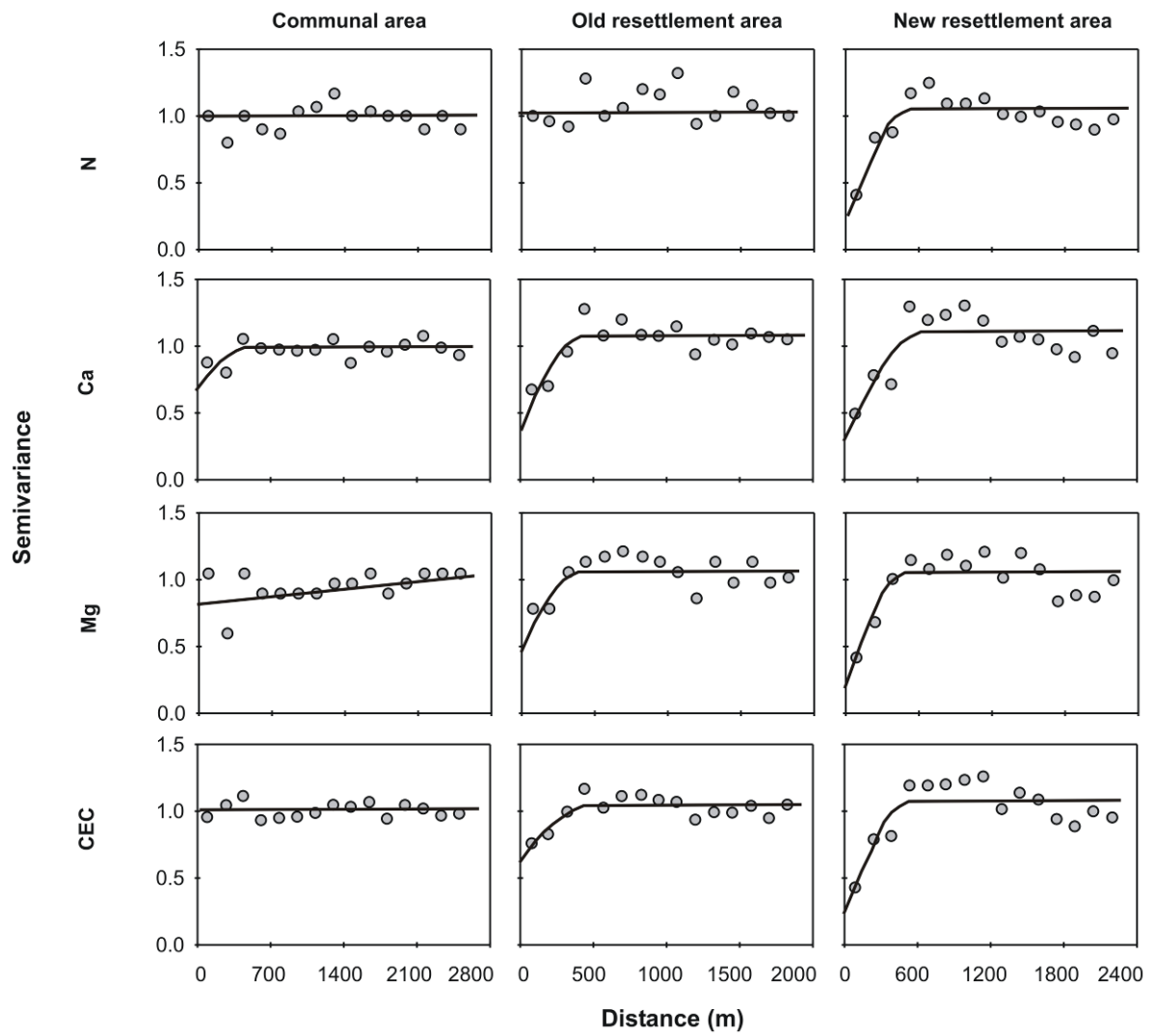
866  
 867  
 868  
 869  
 870  
 871  
 872  
 873

Figure 6. Minimum sample sizes required for estimating the mean of different evaluated soil properties at different probabilities of its true value (margin of error), with a 95% of confidence in: communal area (closed triangles), old resettlement (closed circles) and new resettlement (open circles). Notice that Y-axes are in logarithmic scale. Number of data for calculations and units as shown in Figure 4.



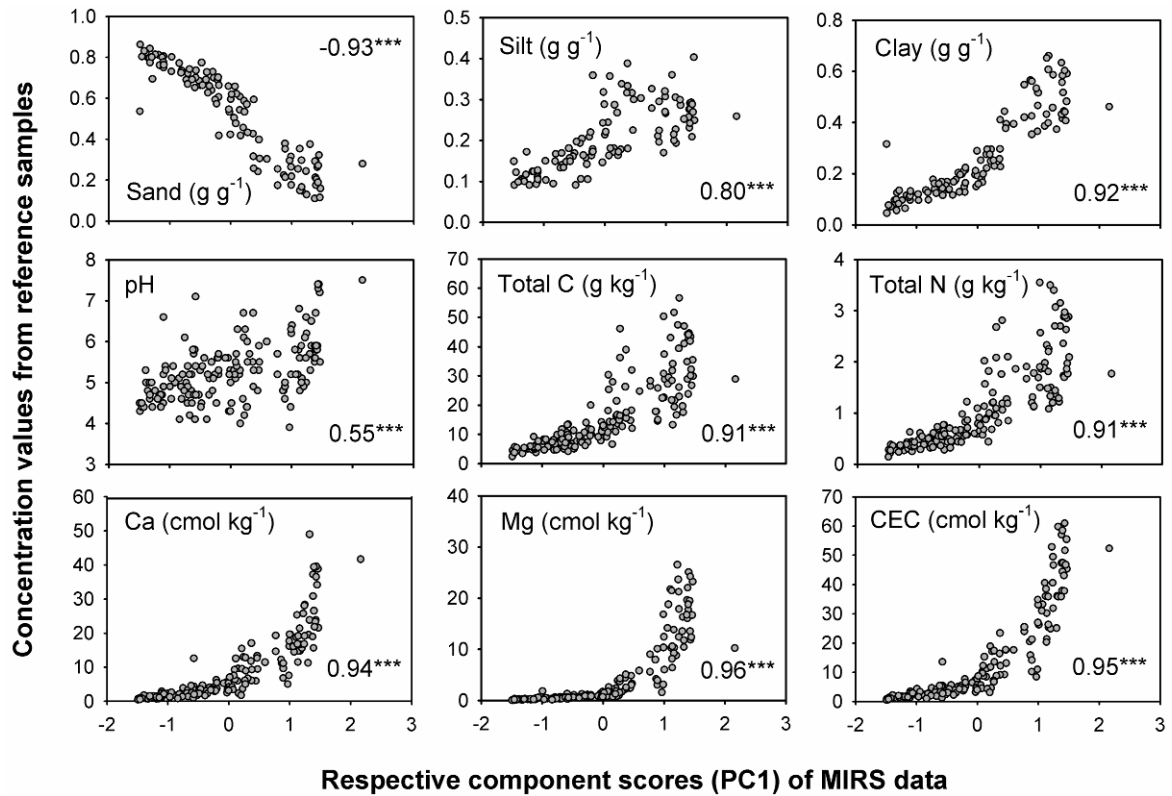
874  
 875  
 876  
 877  
 878  
 879

Figure 7. Standardized experimental (circles) and theoretical (line) semivariograms for evaluated soil properties in the three areas under study. For model parameters please refer to Table 3.



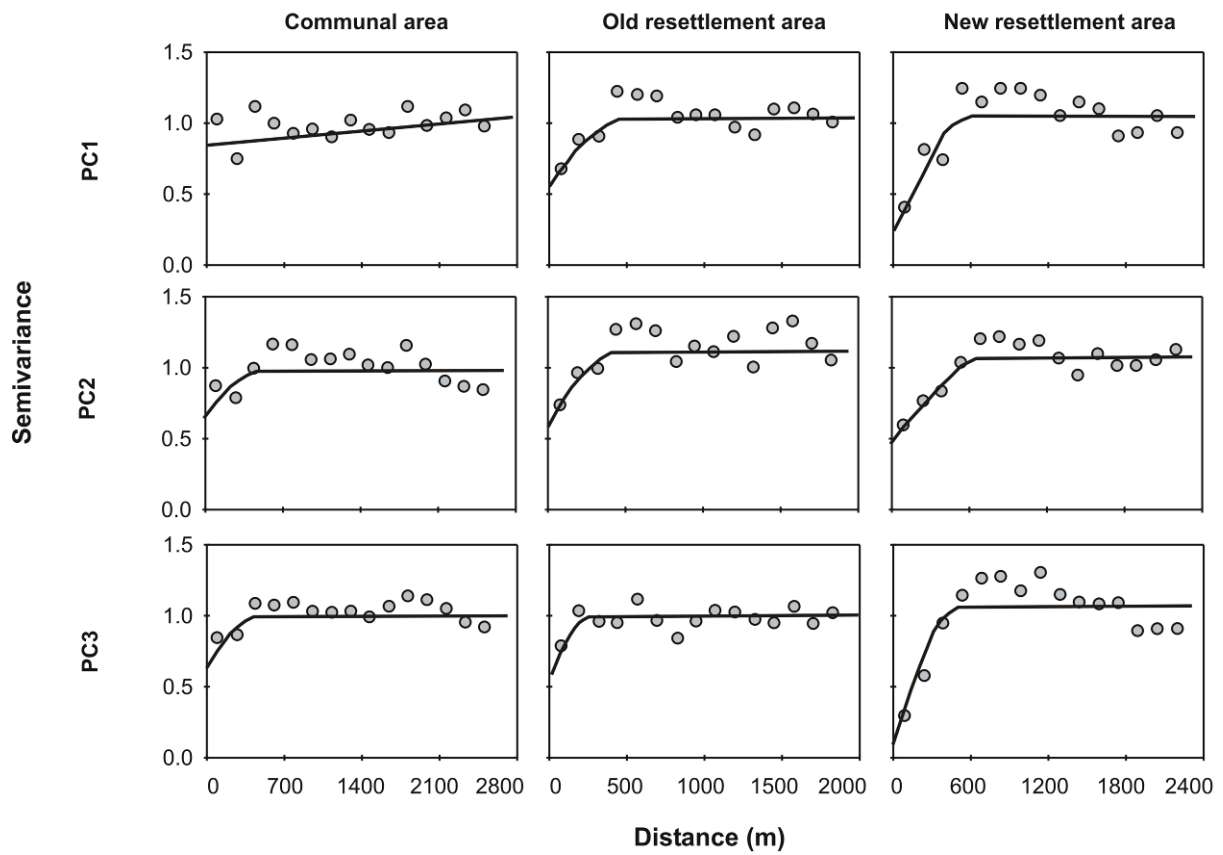
880  
881  
882  
883

Figure 7. Continuation



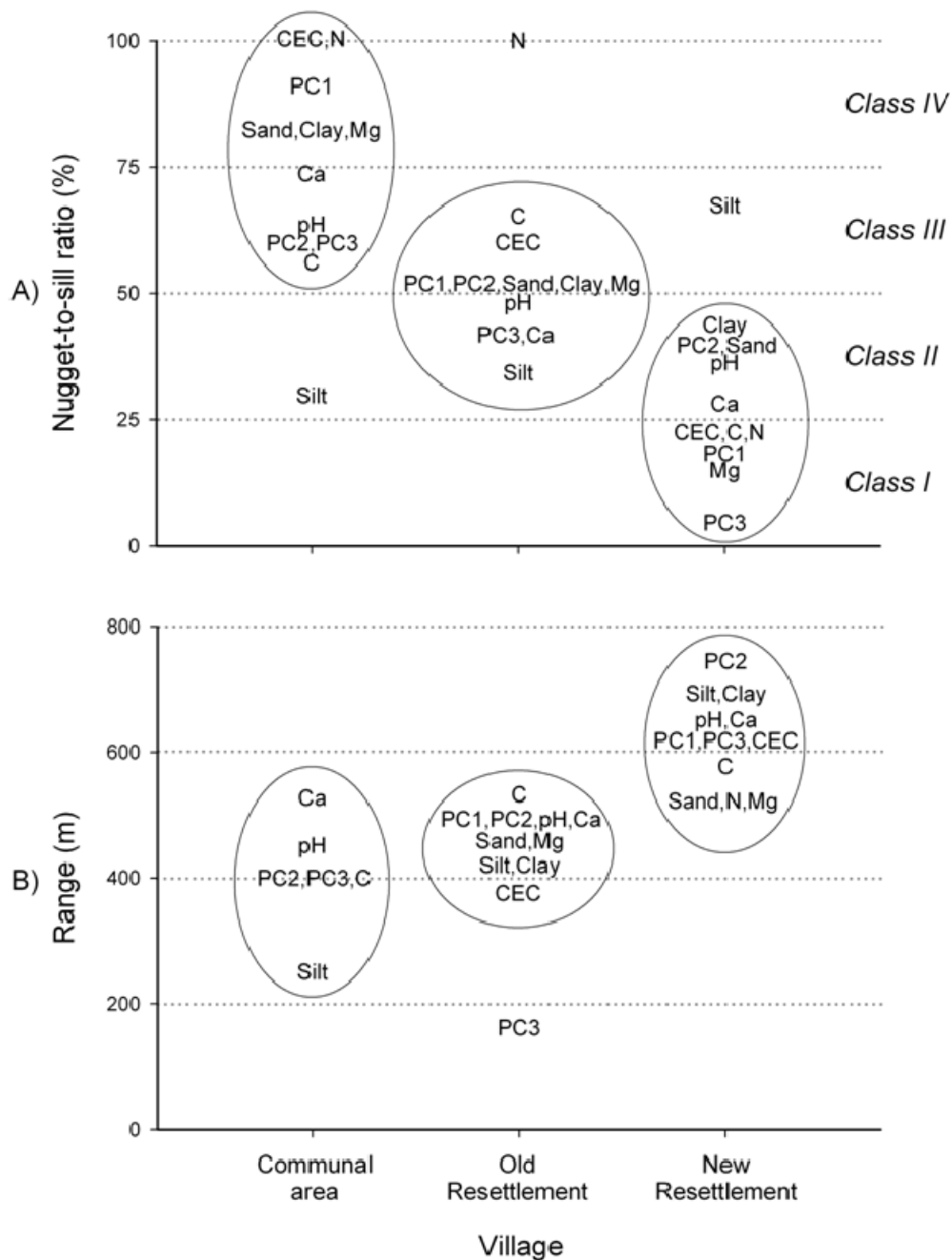
884  
 885  
 886  
 887  
 888  
 889  
 890  
 891

Figure 8. Scatter plots and Spearman correlation coefficients for the relationships between soil properties from reference samples (i.e. analyzed by conventional laboratory procedures) and respective component scores of the first principal component (PC1) based on MIRS data. \*\*\*:  $p < 0.001$ .



892  
 893  
 894  
 895  
 896  
 897

Figure 9. Standardized experimental (circles) and theoretical (line) semivariograms for the three first principal components based on MIRS data from all soil samples collected in the three areas under study. For model parameters please refer to Table 4.



898

899

900 Figure 10. Comparison of A) nugget-to-sill ratios (and spatial dependency classes as defined  
 901 in the text), and B) ranges, from semivariograms of the three studied settlement schemes  
 902 based on MIRS-derived principal components (PC1-PC3) and evaluated soil properties.

903 Circles exclude variables that deviate from the behavior of the main group. Variables with

904 undefined ranges (see Tables 3 and 4) were not plotted.